5-18-2023

Influenza C and D Viruses Demonstrated a Differential Respiratory Tissue Tropism in a Comparative Pathogenesis Study in Guinea Pigs

Chithra C. Sreenivasan

Runxia Liu

Rongyuan Gao

Yicheng Guo

Ben M. Hause

See next page for additional authors

Authors

Chithra C. Sreenivasan, Runxia Liu, Rongyuan Gao, Yicheng Guo, Ben M. Hause, Milton Thomas, Ahsan Naveed, Travis Clement, Dana Rausch, Jane Christopher-Hennings, Eric Nelson, Julian Druce, Miaoyun Zhao, Radhey S. Kaushik, Qingsheng Li, Zizhang Sheng, Dan Dan, and Feng Li

AMERICAN SOCIETY FOR MICROBIOLOGY | Journal of Virology®

PATHOGENESIS AND IMMUNITY

Influenza C and D Viruses Demonstrated a Differential Respiratory Tissue Tropism in a Comparative Pathogenesis Study in Guinea Pigs

Chithra C. Sreenivasan,[a] Runxia Liu,[b] Rongyuan Gao,[b] Yicheng Guo,[c] Ben M. Hause,[d] Milton Thomas,[d] Ahsan Naveed,[a] Travis Clement,[d] Dana Rausch,[d] Jane Christopher-Hennings,[d] Eric Nelson,[d] Julian Druce,[e] Miaoyun Zhao,[f,g] Radhey S. Kaushik,[b] Qingsheng Li,[f,g] Zizhang Sheng,[c] Dan Wang,[a] Feng Li[a]

[a]Department of Veterinary Science, M. H. Gluck Equine Research Center, University of Kentucky, Lexington, Kentucky, USA
[b]Department of Biology and Microbiology, South Dakota State University, Brookings, South Dakota, USA
[c]Zuckerman Mind Brian Behavior Institute, Columbia University, New York, New York, USA
[d]Department of Veterinary and Biomedical Sciences, South Dakota State University, Brookings, South Dakota, USA
[e]Virology Section, Victorian Infectious Diseases Reference Laboratory, Melbourne, Victoria, Australia
[f]Nebraska Center for Virology, University of Nebraska—Lincoln, Lincoln, Nebraska, USA
[g]School of Biological Sciences, University of Nebraska—Lincoln, Lincoln, Nebraska, USA

ABSTRACT Influenza C virus (ICV) is increasingly associated with community-acquired pneumonia (CAP) in children and its disease severity is worse than the influenza B virus, but similar to influenza A virus associated CAP. Despite the ubiquitous infection landscape of ICV in humans, little is known about its replication and pathobiology in animals. The goal of this study was to understand the replication kinetics, tissue tropism, and pathogenesis of human ICV (huICV) in comparison to the swine influenza D virus (swIDV) in guinea pigs. Intranasal inoculation of both viruses did not cause clinical signs, however, the infected animals shed virus in nasal washes. The huICV replicated in the nasal turbinates, soft palate, and trachea but not in the lungs while swIDV replicated in all four tissues. A comparative analysis of tropism and pathogenesis of these two related seven-segmented influenza viruses revealed that swIDV-infected animals exhibited broad tissue tropism with an increased rate of shedding on 3, 5, and 7 dpi and high viral loads in the lungs compared to huICV. Seroconversion occurred late in the huICV group at 14 dpi, while swIDV-infected animals seroconverted at 7 dpi. Guinea pigs infected with huICV exhibited mild to moderate inflammatory changes in the epithelium of the soft palate and trachea, along with mucosal damage and multifocal alveolitis in the lungs. In summary, the replication kinetics and pathobiological characteristics of ICV in guinea pigs agree with the clinical manifestation of ICV infection in humans, and hence guinea pigs could be used to study these distantly related influenza viruses.

IMPORTANCE Similar to influenza A and B, ICV infections are seen associated with bacterial and viral co-infections which complicates the assessment of its real clinical significance. Further, the antivirals against influenza A and B viruses are ineffective against ICV which mandates the need to study the pathobiological aspects of this virus. Here we demonstrated that the respiratory tract of guinea pigs possesses specific viral receptors for ICV. We also compared the replication kinetics and pathogenesis of huICV and swIDV, as these viruses share 50% sequence identity. The tissue tropism and pathology associated with huICV in guinea pigs are analogous to the mild respiratory disease caused by ICV in humans, thereby demonstrating the suitability of guinea pigs to study ICV. Our comparative analysis revealed that huICV and swIDV replicated differentially in the guinea pigs suggesting that the type-specific genetic differences can result in the disparity of the viral shedding and tissue tropism.

Editor Bryan RG. Williams, Hudson Institute of Medical Research

Address correspondence to Feng Li, feng.li@uky.edu.

The authors declare no conflict of interest.

Received 7 March 2023
Accepted 26 April 2023
Published 18 May 2023

KEYWORDS Guinea pigs, Influenza C, Influenza D, Tissue tropism, animal models, *in vivo*, influenza, pathogenesis, virulence

Influenza viruses are enveloped, single-stranded, negative-sense viruses classified under the *Orthomyxoviridae* family. Currently, there are four genera designated as alphainfluenza/influenza A (IAV), betainfluenza/influenza B (IBV), gammainfluenza/influenza C (ICV), and deltainfluenza/influenza D (IDV) (1). Compared to IAV and IBV (eight-segmented genomes), ICV and IDV possess only seven segments. Influenza A viruses undergo fast evolutionary changes (antigenic shift) and exist as multiple subtypes based on different combinations of the HA and NA segments. However, IBV, ICV, and IDV have a relatively slower evolutionary rate (antigenic drift) and diverge into distinct lineages based on their antigenic and phylogenetic properties (2–4). Influenza B virus diverged into two major lineages. Both ICV and IDV diverged into six and four lineages respectively (5, 6). IAV and IDV types exist in multiple mammalian species with primary reservoirs as aquatic birds and cattle respectively, whereas humans are the primary reservoirs for IBV and ICV.

Influenza D virus (IDV) originally isolated from the swine (7), was widespread in bovine herds and these influenza D viruses share 50% amino acid identity with influenza C viruses, which are primarily human pathogens (8). Despite the sequence identity, IDV cannot undergo gene reassortment with ICV and hence is genetically and antigenically distinct from ICV. Although IDV was initially reported from North America, it was found to have a transboundary occurrence in swine and bovine populations across Eurasia and Africa. A striking feature of IDV is its broad host tropism with multiple mammalian hosts as in small ruminants (goats and sheep), buffaloes, equines, and camelids (9–15). Interestingly, Influenza D antibodies were also present in the occupational workers of the USA (16) and in the archived samples in Italy, before its initial detection in 2011 (17, 18) which implicate the public health importance of influenza D. Further, the IDV genome was detected in the nasal sample of a pig farm worker from Malaysia and also in bioaerosol samples derived from hospitals and airports (19, 20). Compared to influenza A and B viruses, ICV infections are not associated with seasonal epidemics. The multiple lineages of ICV co-circulate and undergo frequent reassortment causing disease in humans (21) and ICV infections are often associated with co-infections involving bacteria and viruses such as adeno, rhino, boca, and respiratory syncytial viruses which complicates to assess its real clinical significance (22). Influenza C virus was first isolated from the throat washings of an ailing man in New York, USA in 1947 (23), even though serological evidence suggests that ICV was prevalent before 1947 (24). While ICV is associated with an acute respiratory illness in children, and is clinically significant in pediatric and community acquired pneumonia (CAP) in different parts of the world (25–41), it causes a mild respiratory disease in adult humans and coexists with IAV and IBV infections (30, 42, 43). Despite the ubiquitous nature of ICV, with 80% of humans harboring antibodies during their early life and the increasing antibody titers by age (24, 42, 44–53), it is generally thought that ICV is an underestimated, yet clinically relevant virus causing the upper respiratory tract (URT) infections in adult humans and the lower respiratory tract (LRT) infections in children.

The spillover of ICV from its principal host, humans to other species, and the level of sequence identity of animal-origin ICV to the human ICV strains suggests the possibility of reverse zoonosis. ICV has been isolated from natural infections of agricultural/companion animals such as cattle, pigs, and dogs (54–62) and serosurveillance studies reported a higher hemagglutination inhibition (HI) antibody titer in pigs and dogs, respectively (62, 63). Seroprevalence of ICV was also reported in dromedary camels in Africa (12). Previous studies revealed that several human ICV strains were antigenically closely related to ICVs reported in pigs (2, 64), and bovines (55, 65), supporting a notion of interspecies transmission, despite the directionality of the transmission that is still inconclusive and needs to be addressed in future studies (2, 66).

Several studies have shown that IDV and ICV evolved to co-exist in pigs, cattle, and humans as suggested by the recent reports of bovine IDV genome detection in human

respiratory samples and detection of human ICV in bovines (19, 55, 56). Bovines harbor both ICV and IDV and it was also reported that both these seven-segmented influenza viruses have key roles in the development of bovine respiratory disease (67). Like ICV, IDV also uses the HEF protein, for the virus entry and exit, and these proteins share a conserved enzymatic site and divergent receptor binding sites. IDV exhibits a broad host tropism, and IDV-HEF has exceptional acid and thermal stability compared to ICV (68). Since both ICV and IDV bind to *9-O* acetylated sialic acids (69, 70), a comparative analysis in an animal model will help to understand replication fitness, tissue tropism, and the pathobiological differences between these two seven-segmented influenza viruses. The primary focus of this study was to study the replication and pathology of these two viruses: IDV and its distant relative ICV, in a guinea pig model. Several studies using small and large animal models have been performed on IDV previously (7, 71–73). DBA/2 mice were used to study D/bovine/France/5920/2014 (D/OK-like) and there was productive viral replication in the URT and LRT despite no clinical signs/weight loss occurring in infected mice (72). Ferrets infected with D/swine/Oklahoma/1334/2011 shed virus in the URT (7). We chose guinea pigs for our study because guinea pigs have been used as an animal model for IAV and IBV studies. Furthermore, our previous studies have demonstrated that guinea pigs could be a good model to study the replication fitness, transmission, and pathogenesis of ICV-related IDV (71, 74). Guinea pig model also offer additional advantages such as cost-effectiveness and ease of handling, compared to dogs and pigs, which are also secondary hosts for ICV. Finally, the guinea pig respiratory tract possesses airway hyperresponsiveness (75) and bronchus associated lymphoid tissue (76), akin to humans.

In this study, we used C/Victoria/2/2012 and D/swine/Oklahoma/1334/2011 as representative strains of ICV and IDV, respectively. The results of our study demonstrated that guinea pigs possess *9-O*-acetylated sialic acid receptors in the upper and lower respiratory tracts and IDV replicated in the URT tissues such as nasal turbinates, and soft palate. Interestingly, we noted ICV replication in the trachea, but not in the lung. On the contrary, swIDV demonstrated more robust replication kinetics in the tissues and nasal washes of the guinea pigs showing a tropism toward both the upper and lower respiratory tracts of the guinea pigs, compared to huICV. Taken together, the data we obtained will support the utility of guinea pigs to study ICV and IDV which can be further explored to illuminate the key factors responsible for the differential tropism of these two related influenza viruses.

RESULTS

Influenza C virus has limited growth at 37°C. To determine the tissue tropism of the ICV *in vitro*, we conducted a replication kinetics study of C/Victoria/2/2012 in species-specific cell lines such as Madin Darby canine kidney (MDCK), swine testicle (ST), and human lung adenocarcinoma cell line (Calu-3) at two different temperatures: 33°C and 37°C simulating the upper and lower respiratory tracts, respectively. MDCK and ST cells were infected at a multiplicity of infection (MOI) of 0.01, while Calu-3 was infected at 1.0 MOI. After infection, samples were collected every 24 h. The samples were titrated on MDCK cells and the titers were determined using the Reed and Muench assay (77). Temperature-dependent virus kinetic study revealed a limited growth of ICV at 37°C in all the cell lines compared to 33°C (Fig. 1). The results of the replication kinetics study indicated that ICV replicated to higher titers at a lower temperature but its replication was limited at a higher temperature.

***9-O*-acetylated sialic acids are present in the guinea pig upper and lower respiratory tract tissues.** Previous studies have shown that both ICV and IDV bind to *9-O*-acetylated sialic acids (69, 70, 78–81). To determine the presence of ICV receptors in the respiratory tissues of guinea pigs, high-performance liquid chromatography (HPLC) was conducted on the cryopreserved tissues of the nasal turbinates, soft palate, and lungs to quantify the amount and type of the sialic acids present. HPLC analyses revealed that a high amount of *N*-Acetylneuraminic acid (Neu5Ac) is present in the nasal turbinates, soft palate, and the lungs, along with a reasonably good amount of *N*-glycolylneuraminic acid (Neu5Gc).

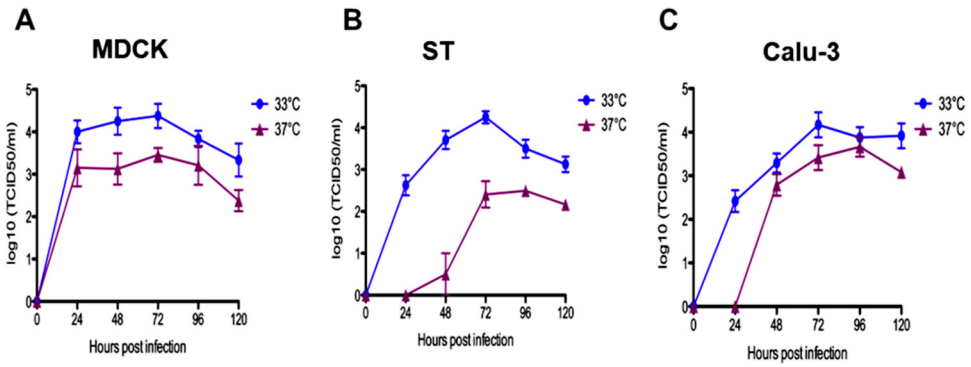

FIG 1 Growth kinetics of C/Victoria/2/2012 in different cell lines at 33°C and 37°C. MDCK, ST and Calu-3cells were infected with C/Victoria/2/2012 and incubated at 33°C and 37°C to represent the upper and lower respiratory tract temperatures, respectively. MDCK, and ST cells were infected with C/Victoria/2/2012 at an MOI of 0.01, while Calu-3 cells were infected at an MOI of 1.0. Samples were collected at 24h intervals and viral titers were determined by 50% tissue culture infective dose assay by titrating the samples on MDCK cells. Virus replication kinetics of C/Victoria/2/2012 for (A) MDCK (B) ST and (C) Calu-3 at 33°C and 37°C are shown. The values shown are mean ± SEM and plotted as a function of time.

Besides Neu5Ac and Neu5Gc, the guinea pig respiratory tract also expresses *9-O*-acetylated sialic acids such as Neu5,9Ac2 (acetyl group at C5 and C9 positions), Neu5Gc9Ac (acetyl position at C9 and glycolyl group at C5 positions), which are two predominant receptors for ICV and IDV entry. The HPLC chromatograms and the levels of total sialic acid and *9-O*-acetylated sialic acids expressed in *pmol* for each tissue are summarized in Fig. 2A and B. The rank order of Neu5,9Ac2 levels in respiratory compartments was lungs>nasal turbinate>soft palate whereas the order for Neu5Gc9Ac levels was lungs>soft palate>nasal turbinate. Taken together, *9-O* acetyl sialic acids, particularly Neu5,9Ac2 (the receptor of ICV), are present in all three tissues lining the upper and lower respiratory tracts at appreciable levels, further confirming that guinea pigs could be used to study the replication fitness and tropism of ICV.

Experimental design, clinical signs, changes in body weight and temperature. To study the replication fitness and pathogenesis of huICV, we inoculated guinea pigs intranasally with C/Victoria/2/2012 and compared its pathobiological correlates to its distant relative D/swine/1334/2011. A schematic representation of the experimental design is shown in Fig. 3A. Twenty-five ICV/IDV antibody-negative Dunkin-Hartley guinea pigs were divided into three groups and intranasally inoculated with 3 x10^5 $TCID_{50}$/0.3 mL of C/Victoria/2/2012 (huICV, *n* = 10), D/swine/1334/2011 (swIDV, *n* = 10), and mock (PBS, *n* = 5). Animals were acclimatized for 1 week and screened for any ICV or IDV antibodies again before the virus inoculation. After inoculation, the nasal washes were collected from the virus and mock-infected animals on 1, 3, 5, and 7 dpi. Two animals were euthanized from the virus-infected groups on these days to collect blood and tissues for studying virus replication kinetics and tissue tropism. The number of animals sampled for nasal washes in the huICV and swIDV infected groups is 10 at 1 dpi, 8 at 3 dpi, 6 at 5 dpi, and 4 at 7 dpi. Nasal washes sampled from the mock group are *n* = 5 for 1, 3, 5, and 7 dpi. Three animals from the mock-infected group were euthanized on 7 dpi. Two animals were maintained in all the groups till 14 dpi to test seroconversion. Body weights and temperature were measured from 2 days prior to the inoculation till the end of the animal experiment.

The guinea pigs after the inoculation of huICV did not develop any clinical signs and the animals behaved normally. For each animal, the change in body weight postinfection was calculated by comparing the postinfection body weight on each day to the average of the body weights recorded 2 days before the infection. The differences were calculated individually for all the animals in the group and the average percentage change in body weight was plotted for each day. Animals directly inoculated with swIDV also did not show any significant change in body weight compared to the mock-infected animals (Fig. 3B). Similarly, the difference between the postinfection body temperature and the pre-infection

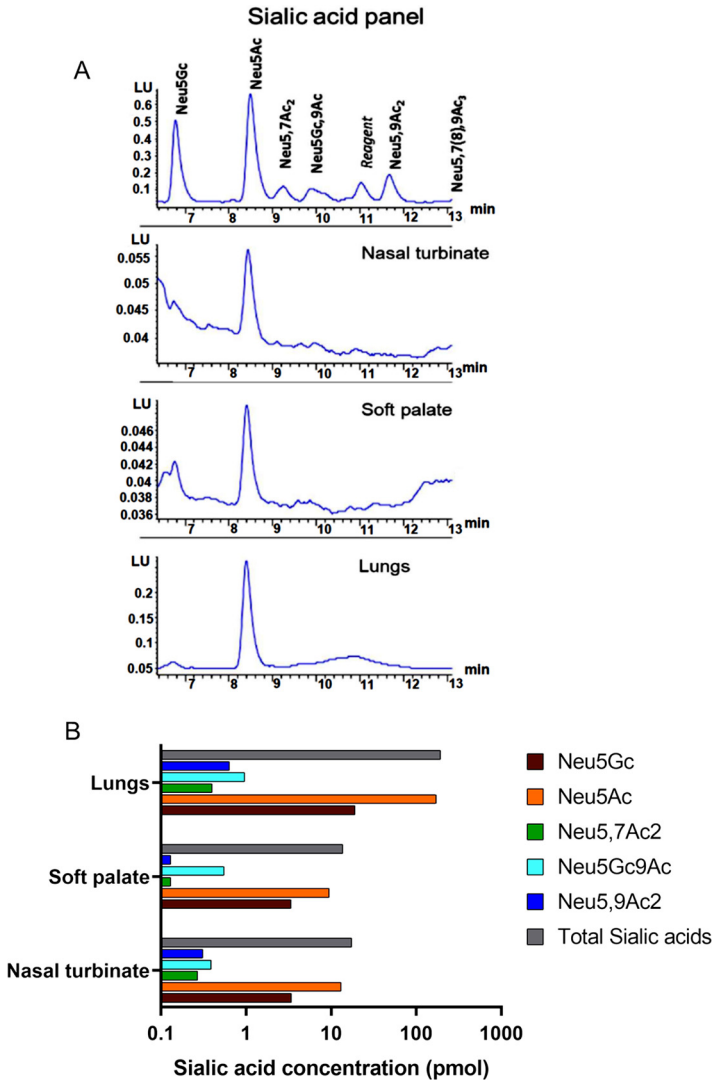

FIG 2 Presence of 9-O-acetylated sialic acids in the upper and lower respiratory tract of the guinea pigs by high-performance liquid chromatography (HPLC). Frozen guinea pig respiratory tissues such as nasal turbinate, soft palate and lungs were processed to separate the sialic acid portion on the membrane and then analyzed to determine the concentration of different types of sialic acids. (A) Reference sialic acid panel used for the analyses of guinea pig tissues and the HPLC chromatograms for each tissue (B) Sialic acid concentration expressed in *pmol* for each tissue type.

temperature was determined for each animal, and the mean of differences was plotted for each day (Fig. 3C). Animals infected with both huICV and swIDV showed no significant change in body temperature before and after infection. These results indicated that huICV and swIDV infections did not result in body weight and temperature changes, even though there were virus shedding and pathological changes caused by both viruses during the 14 days of experimental observation as described below.

Growth kinetics and tissue tropism of huICV compared to swIDV in the upper and lower respiratory tracts of guinea pigs. To determine the viral replication fitness of huICV compared to swIDV in the respiratory tract of the guinea pigs, a quantitative analysis of the virus load in the nasal washes was conducted by titrating the samples on MDCK cells to determine the 50% tissue culture infective dose. Nasal washes were collected from the direct inoculated and mock-infected animals at 48h intervals from 1 dpi to 7 dpi (Fig. 4 A-C). The number of animals sampled for nasal washes in the huICV and swIDV infected groups is 10 (1 dpi,) 8 (3 dpi), 6 (5 dpi), and 4 (7 dpi) as mentioned before. It should be noted that the subsequent decrease in the number is due to the two animals being euthanized at every 48 h intervals. Nasal shedding was not

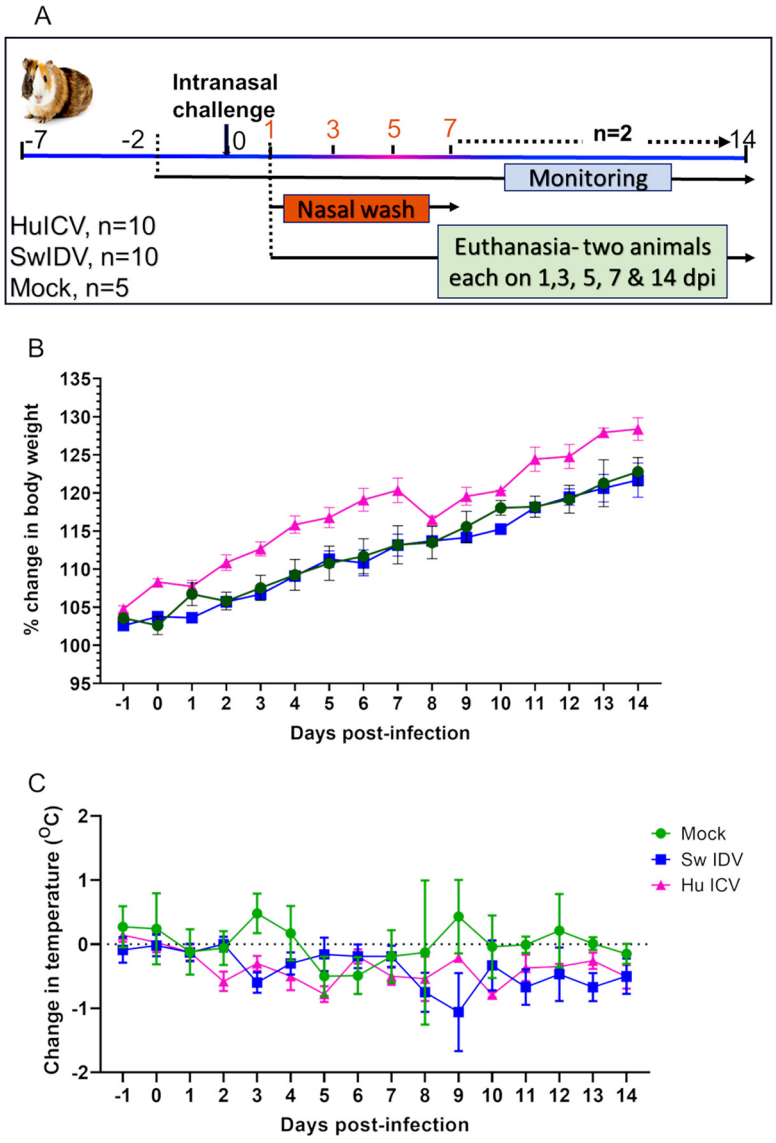

FIG 3 Experimental design, body weight and temperature changes. (A) Schematic diagram of the experimental design of the study. Twenty-five Dunkin-Hartley guinea pigs were divided into three groups and intranasally inoculated with 3x 10^5 $TCID_{50}$/0.3 mL of C/Victoria/2/2012 (huICV, n = 10), D/swine/Oklahoma/1334/2011 (swIDV, n = 10), and mock (PBS, n = 5). After inoculation, the nasal washes were collected from the virus and mock-infected animals on 1, 3, 5, and 7 dpi. Simultaneously, two animals were euthanized from the virus-infected groups on these days to study the virus replication kinetics and tissue tropism. Three animals from the mock-infected group were euthanized on 7 dpi. Two animals were maintained in all the groups till 14 dpi to test seroconversion. Body weights and temperature were measured from 2 days before the inoculation till the end of the animal experiment. (B, C) Body weight and temperature changes in guinea pigs after intranasal inoculation with huICV and swIDV. The change in body weight was calculated by comparing the postinfection body weight on each day to the average of the body weights recorded 2 days before the infection. The individual differences were calculated for all the animals in the group for each day and the mean of percentage changes in body weight was plotted. Similarly, the difference between the postinfection body temperature and the average pre-infection temperature was determined for each animal and a change in the temperature was plotted for each day. (B) Percentage changes in body weight and (C) changes in body temperature were expressed as mean ± standard error (SE) and plotted against the time.

present in both groups on 1 dpi. Out of the 10 animals inoculated with huICV, three animals demonstrated virus shedding in the nasal washes, indicating that huICV was able to infect the guinea pigs, replicate in their respiratory system, and was capable of viral shedding in nasal secretions. Further analysis of the huICV group revealed that 2/8, 2/6, and 1/4 animals shed the virus on 3, 5, and 7 dpi respectively (Fig. 4A).

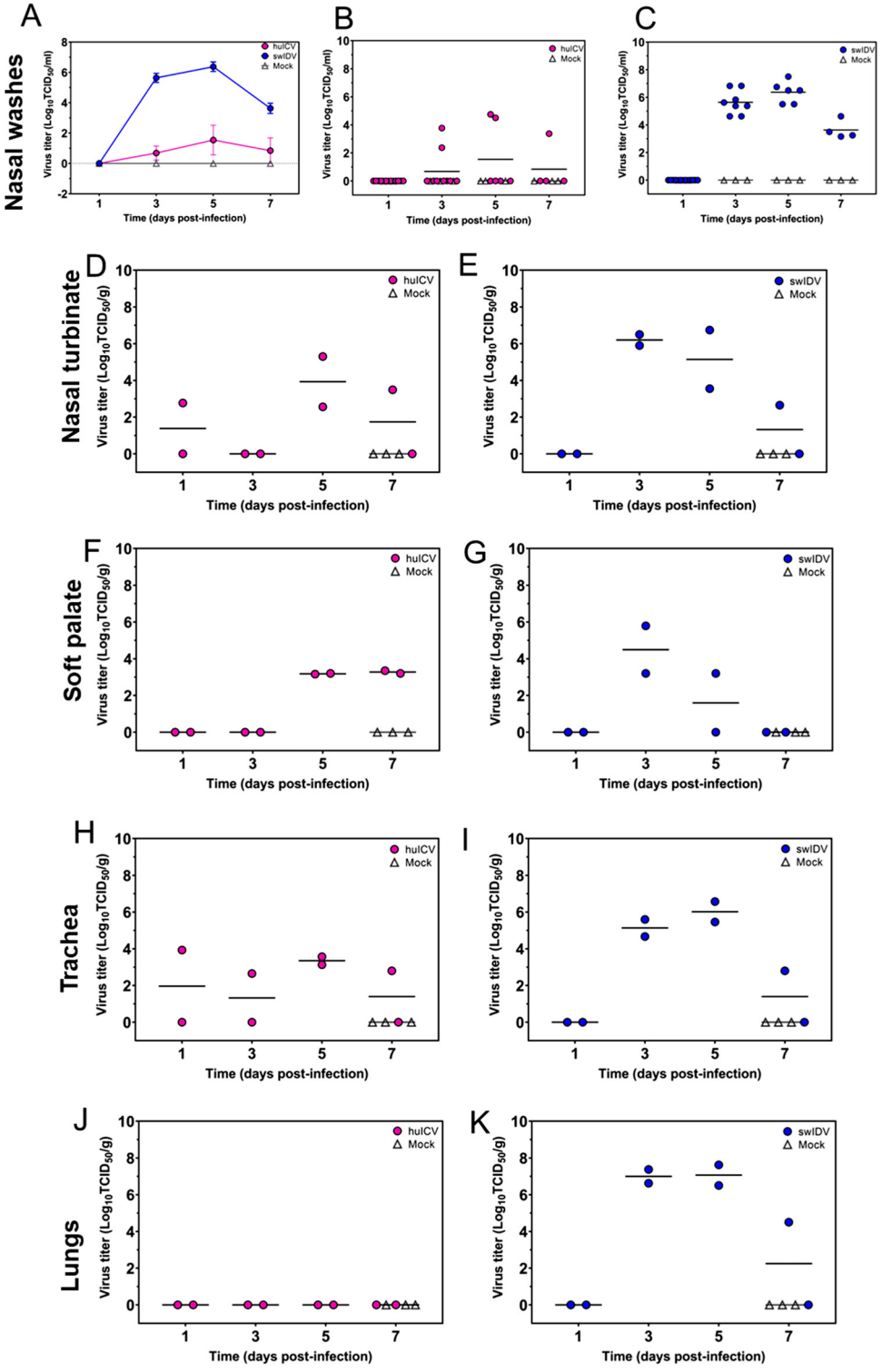

FIG 4 Replication kinetics of huICV and swIDV in nasal washes, and upper respiratory tract (nasal turbinate and soft palate) and lower respiratory tract (trachea and lungs) tissues. Guinea pigs were intranasally inoculated with 3×10^5 $TCID_{50}$/0.3 mL of huICV and swIDV and then nasal washes were collected from animals on 1, 3, 5, and 7 dpi. On these days, two inoculated animals per group were randomly euthanized to assess virus load in the upper respiratory tract tissues such as nasal turbinate, and soft palate. Three mock-inoculated animals euthanized at 7 dpi were also shown. Viral loads in the nasal washes and tissue homogenates were determined by the 50% tissue culture infective dose assay using MDCK cells. Virus titers were expressed as log_{10} $TCID_{50}$ per mL in nasal washes and $log_{10}TCID_{50}$ per gram in nasal turbinate, soft palate, trachea and lungs. Mean viral titers in nasal washes of huICV compared to swIDV along with mockwas shown in (A). Nasal shedding of the

(Continued on next page)

Collectively, 3/10 ICV infected animals demonstrated a productive replication with 2 animals beginning to shed the virus on 3 dpi (2.375, 3.775 logs) and continuing to produce infectious particles on 5 dpi (4.5, 4.75 logs), followed by the termination of virus shedding on 7 dpi. The third animal started virus shedding (3.375 logs) only on 7 dpi, however, this animal was terminated and hence could not track further shedding. The mean viral titers in nasal washes for the huICV-infected animals (including animals detected negative for viral shedding) were 0.68, 1.54, and 0.84 $\log_{10}$ $TCID_{50}$/mL on 3, 5, and 7 dpi (Fig. 4A) respectively with an individual peak titer of 4.75 $\log_{10}$ $TCID_{50}$/mL on 5 dpi (Fig. 4B).

In the case of swIDV, eight out of 10 inoculated animals shed the virus indicating that robust replication occurred in the respiratory tract of the guinea pigs. The nasal wash sampling scheme of swIDV is the same as the huICV group (Fig. 3A). We found that 8/8, 6/6, and 4/4 swIDV infected animals shed virus on 3, 5, and 7 dpi respectively (Fig. 4C). Despite no viral shedding on 1 dpi in the swIDV group, the mean viral titers were 5.64, 6.38, and 3.63 $\log_{10}$ $TCID_{50}$/mL for infected animals on 3, 5, and 7 dpi respectively (Fig. 4A), with an individual peak titer of 7.5 $\log_{10}$ $TCID_{50}$/mL on 5 dpi (Fig. 4C). For both groups, the peak shedding occurred on 5 dpi. Mock animals did not have any detectable virus at any time point throughout the 2-week study.

To study the tissue tropism of huICV, two animals were randomly selected and euthanized on 1, 3, 5, and 7 dpi, and nasal turbinate, soft palate, trachea, and lung were collected to test the tissue tropism in the lower and upper respiratory tracts. Similarly, three animals from the mock-infected group were also euthanized on 7 dpi and the tissues were collected. The soft palate shares the junctional site with the nasopharyngeal and oral surface, which is considered previously a key spot for the influenza A virus adaptation (82). As such, the soft palate was collected to study the comparative tropism of huICV and swIDV. In both groups, the tissue homogenates from the nasal turbinate, and the soft palate showed appreciable viral titers from 1 dpi through 7 dpi, confirming that both ICV (Fig. 4D, and F) and IDV (Fig. 4E, and G) productively replicated in the URT. In the case of huICV, the number of animals with detectable virus load in tissue homogenates at different time points (dpi in bold) was as follows: nasal turbinate—1**dpi**-1/2, 3 **dpi**-0/2, 5 **dpi**-2/2, 7 **dpi**-1/2 and soft palate—1**dpi**-0/2, 3 **dpi**-0/2, 5 **dpi**-2/2, 7 **dpi**-2/2 whereas in the swIDV group, nasal turbinate—1**dpi**-2/2, 3 **dpi**-2/2, 5 **dpi**-2/2, 7 **dpi**-1/2; and soft palate—1**dpi**-0/2, 3 **dpi**-2/2, 5 **dpi**-2/2, 7 **dpi**-0/2, showed detectable virus loads. The presence of huICV in the nasal turbinate on 1 dpi but absent on 3 dpi in both animals is indicative of the residual virus from the inoculum. In nasal turbinate, the peak huICV mean titer was 3.93 $\log_{10}$ $TCID_{50}$/g on 5 dpi, while swIDV mean titer was 6.2 $\log_{10}$ $TCID_{50}$/g on 3 dpi. In the soft palate, huICV mean titers were 3.18 and 3.28 $\log_{10}$ $TCID_{50}$/g on 5 and 7 dpi respectively while swIDV was able to replicate productively with a peak mean titer of 4.5 $\log_{10}$ $TCID_{50}$/g on 3 dpi. On 7 dpi, huICV-infected animals continued to have a virus load in the soft palate, while there was no virus load in swIDV-infected animals (Fig. 4F, and G).

To study the tissue tropism toward the lower respiratory tract, virus load in the trachea and lung homogenates was determined by the 50% tissue culture infective dose assay (Fig. 4H-K). For huICV, the number of animals with detectable viral load in the LRT tissues at different time points (dpi in bold) was as follows: trachea—1**dpi**-1/2, 3 **dpi**-1/2, 3 **dpi**-2/2,7 **dpi**-1/2 and lungs—1**dpi**-0/2, 3 **dpi**-0/2, 3 **dpi**-0/2, 7 **dpi**-0/2 (Fig. 4H, and J) whereas in swIDV: trachea —1**dpi**-0/2, 3 **dpi**-2/2, 5 **dpi**-2/2, 7 **dpi**-1/2 and lungs—1**dpi**-0/2, 3 **dpi**-2/2, 5 **dpi**-2/2, 7 **dpi**-1/2, showed detectable virus loads (Fig. 4I, and K). Human ICV was able to replicate in the trachea with a peak mean titer of 3.35 and 1.4 logs on 5 and 7 dpi, however, there was no detectable virus load in the lungs.

FIG 4 Legend (Continued)

guinea pigs postinfection was shown by plotting individual viral titers of huICV (B) and swIDV (C). Virus titers/loads detected in nasal turbinate of huICV(D) and swIDV (E); in soft palate of huICV(F) and swIDV (G); in trachea of huICV(H) and swIDV (I) and lungs of huICV(J) and swIDV (K). For all the panels, each shape represents an individual animal and horizontal bars show the mean viral titers for each time point.

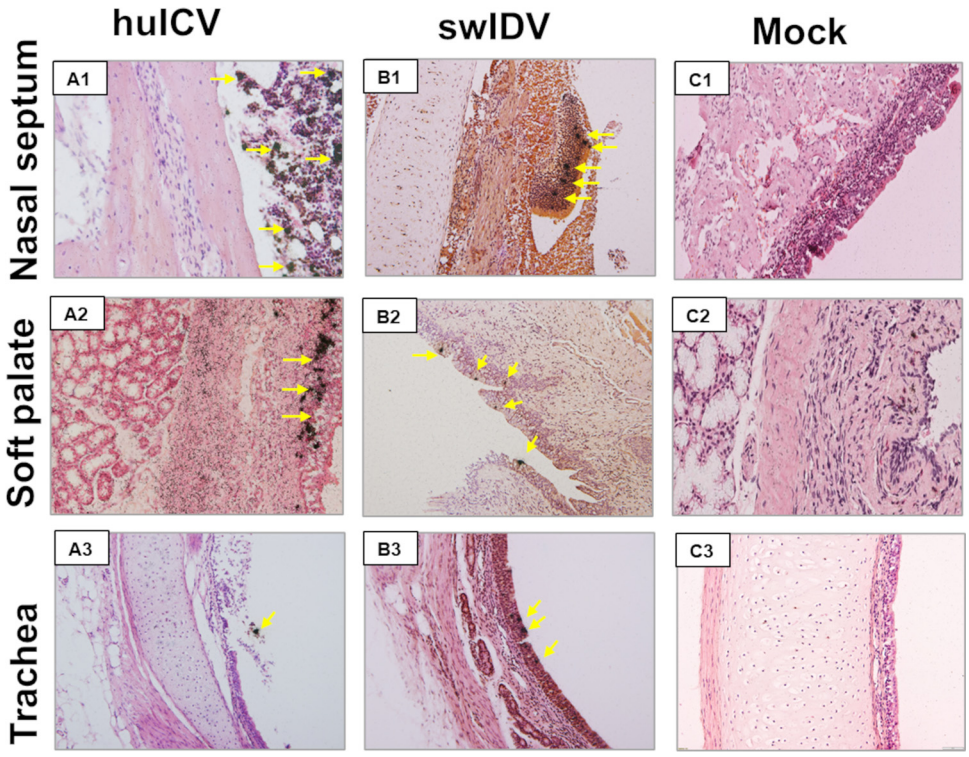

FIG 5 Tissue tropism determined by viral RNA localization by ISH in respiratory tissues of guinea pigs. To confirm the tropism of the viruses, ISH assay was conducted on the mid-nasal septum, soft palate, and trachea at different time points. Representative images of huICV (A1-3), swIDV (B1-3) at 5 dpi, and mock (C1-3) at 7 dpi were demonstrated in the left, middle, and right panels, respectively. ICV-specific RNAs were visible as black silver grains in the radioautographs and seen localized to the epithelial cells lining the mid-nasal septum, soft palate, and trachea. (A1) mid-nasal septum, (A2) soft palate, and (A3) trachea of huICV-infected animals. IDV-specific RNAs present along the epithelial cells lining of (B1) mid-nasal septum, (B2) soft palate, and (B3) trachea were shown with the same visible color as that used for ICV RNAs.

Compared to huICV, swIDV replicated to a mean peak titer of 6 $\log_{10}$ $TCID_{50}$/g in the trachea (5 dpi) and 7 $\log_{10}$ $TCID_{50}$/g in the lungs on both 3 and 5 dpi (Fig. 4I, and K). Taken together, both huICV and swIDV did not show virus load on 1 dpi in both upper and lower respiratory tracts. Human ICV demonstrated the preferential tropism to the URT tissues over the lower respiratory tract, while swIDV demonstrated a broad tissue tropism to both upper and lower respiratory tracts with appreciable viral titers at all time points. Another striking feature is that the soft palate had a prolonged huICV presence till 7 dpi, indicating that huICV has relatively longer viral persistence compared to swIDV, which got cleared by 7 dpi. Mock animals did not show any virus in all the assayed tissues at any time points.

Presence of viral RNA (vRNA) in tissues confirmed by *in-situ* RNA hybridization. To confirm the tissue tropism, we also conducted *in-situ* RNA hybridization (ISH) to locate the vRNA in different tissues of URT and LRT, using sulfur (^{35}S)-labeled negative-sense RNA probe derived from viral nucleoprotein (NP) of the respective viruses. The ISH clearly revealed vRNAs of huICV distributed in the lining epithelial cells of the mid nasal septum, soft palate, and trachea (Fig. 5A1, A2, and A3), but not in the lungs (Fig. 6A1, A2, and A3). However, swIDV RNA was detected in the epithelial cells of all respiratory tissues in the URT (Fig. 5B1, B2, and B3) and LRT (Fig. 6B1, B2, and B3). In the lungs, swIDV RNA was localized in the lining epithelial cells of the bronchioles (enlarged inset picture). Similar to the virus load results, tissues from 5 dpi showed increased localization of the vRNAs in both virus groups (Fig. 5, and 6). No ICV RNA was detected in the lungs by ISH, thus confirming that huICV does not show lung tropism and has a predilection toward the URT tissues, while swIDV demonstrated robust viral replication in both upper and lower respiratory tract tissues, with a substantial peak titer in the lungs, thus confirming its broad cell tropism. The

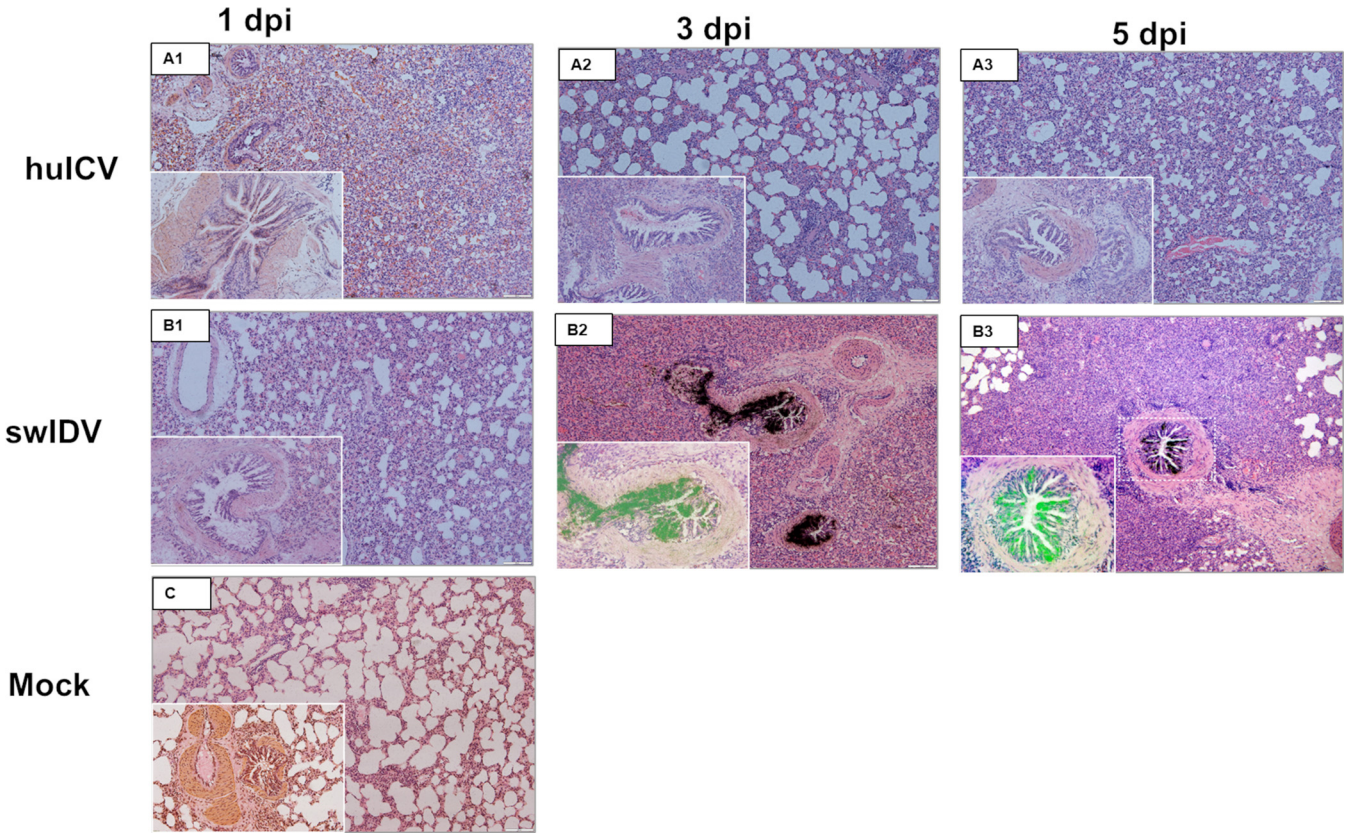

FIG 6 Viral RNA localization in lung tissues by ISH. To confirm the cell tropism of the viruses, an ISH assay was conducted on lung tissues at 1, 3, and 5 dpi, ICV (top), and IDV (bottom). (A1-3) ICV RNAs were not detected in lung parenchyma and bronchiolar epithelial cells at all the time points tested. (B1-3) IDV-specific RNAs were visible as black silver grains in the radioautographs in the lung tissues of swIDV-infected animals at 3 and 5 dpi, but not at 1 and 7 dpi. IDV RNAs were seen localized to the bronchial epithelial cells in the swIDV-infected lungs. Insets represent bronchioles with viral RNA deposition (green grains) under an epipolarized microscope. ICV RNAs were not detected in lung parenchyma and bronchiolar epithelial cells at all time points. (C) the lung from the mock animal at 7 dpi.

results obtained from ISH correlated nicely with the virus isolation, thus confirming the tropism and replicative fitness of huICV and swIDV as observed in the viral isolation approach.

RNA sequencing analysis of the viral transcriptomes in lungs. From the data above, it was evident that the huICV and swIDV, both with no appreciable viral shedding/load on 1 dpi in nasal washes, demonstrated a differential pattern of replication and virus shedding in guinea pigs. The viral genome and protein sequence changes that occurred in the guinea pig URT were further determined by performing deep RNA sequencing of the viruses from the nasal washes at 5 dpi and compared to the parent inoculum (Table 1). For huICV, non-synonymous mutations were observed in viral polymerase P3 (E508K, T577P, V592L), HEF (A182T, R502K), and M (E90G, M122K) segments, while PB2, PB1, NP, and NS segments did not exhibit any mutations (Table 1). Deep RNA sequencing of the nasal wash from swIDV infected guinea pig (5 dpi) exhibited mutations in the viral genome segments PB2, PB1, P3, HEF, NP, and NS (Table 2). While amino acid changes were noticed only in the NS (D285A) segment, others were synonymous mutations (Table 2.).

To further confirm the peculiar replication pattern observed in these two virus groups, we conducted RNA-Seq analyses on lung tissues of huICV and swIDV infected animals from 1, 3, and 5 dpi and compared the viral transcriptome to the inoculum. RNA-Seq analysis enabled us to examine whether huICV has a lung tropism in guinea pigs and to determine any possible mutations for swIDV that may have facilitated viral adaptation promoting high viral titer. As expected, the expression of huICV genes was not present at all time points in the lungs, however, swIDV transcriptomes were present in the lungs of infected guinea pigs on 3 and 5 dpi (Fig. 7). These results were in perfect agreement with our virus isolation and ISH data. The normalized read counts

TABLE 1 Changes in the viral genome and proteins of ICV derived from the nasal washes of the huICV infected guinea pig (5 dpi) compared to inoculum[a]

	hICV inoculum *Vs* nasal wash			
Segment	**Position**	**Nucleotide substitutions**	**Position**	**Amino acid substitutions**
P3	1544	G-A	508	E-K
	1751	A-C	577	T-P
	1801	G-C	592	V-L
HEF	567	G-A	182	A-T
	1336	C-A		
	1528	G-A	502	R-K
	1532	T-C		
M	295	A-G	90	E-G
	391	T-A	122	M-K

[a]No mutations observed in PB2, PB1, NP, and NS segments.

for PB2, PB1, P3, HEF, NP, P42, and NS genes for swIDV and huICV wasgiven in Fig. 7A. The positional read depth for the seven segments of swIDV in infected animals at 3 and 5 dpi was provided in Fig. 7B. RNA-Seq experiment also demonstrated that swIDV genome replicated in lungs and the results obtained was comparable with the viral 50 percent tissue culture infectivity ($TCID_{50}$) experiment (Fig. 4). Further sequence analysis of the viral transcriptomes showed no detectable amino acid changes in the genes of swIDV, indicating that IDV can directly replicate in and adapt to the lungs of guinea pigs without evolving mutations.

Gross lesions and histopathology. Human ICV-infected guinea pigs did not show any appreciable gross lesions in the URT tissues (Fig. 8A,D, and G), however, the histopathological analyses revealed mild to moderate inflammatory changes with mucosal disruption in the lining epithelium of the soft palate and trachea by 5 and 7 dpi respectively (Fig. 8D, and G). In the huICV group, there was moderate infiltration of lymphocytes and plasmacytic cells in the submucosa of the trachea and soft palate on 5 and 7 dpi (Fig. 8D, and G).

Despite lacking evidence of ICV in lungs, huICV-infected guinea pig lungs showed mild to moderate changes macroscopically, characterized by areas of congestion and hemorrhage on 1 dpi which eventually progressed to areas of pulmonary consolidation on 3 and 5 dpi (Fig. 9A, cyan arrowheads). Histopathological examination of lungs from huICV-infected animals showed mild to moderate atelectasis, multifocal areas of inflammation characterized by infiltration of inflammatory cells such as neutrophils, lymphocytes, and RBCs in the lung parenchyma with a thickened alveolar septum, and mild changes in the bronchioles without much epithelial denudation (Fig. 9C1-C4). Lungs from mock-infected animals did not show pneumonic/consolidative lesions (Fig. 9E).

Similar to huICV, swIDV-infected animals also demonstrated no appreciable gross lesions for URT tissues. However, histopathological analyses revealed moderate inflammatory changes along the mucosa and lymphoplasmacytic infiltrations in the submucosa of the soft palate and trachea as shown in Fig. 8E and H. Mid nasal septum also showed mild

TABLE 2 Changes in the viral genome and proteins of IDV derived from the nasal washes of the swIDV infected guinea pig (5 dpi) compared to inoculum[a]

	swIDV inoculum Vs nasal wash			
Segment	**Position**	**Nucleotide substitutions**	**Position**	**Amino acid substitutions**
PB2	845	A-G		
	848	T-C		
PB1	578	A-G		
	678	G-A		
P3	493	A-G		
HEF	1048	C-T		
NP	1278	A-G		
NS	861	A-C	285	D- A

[a]No mutations observed in P42 segment.

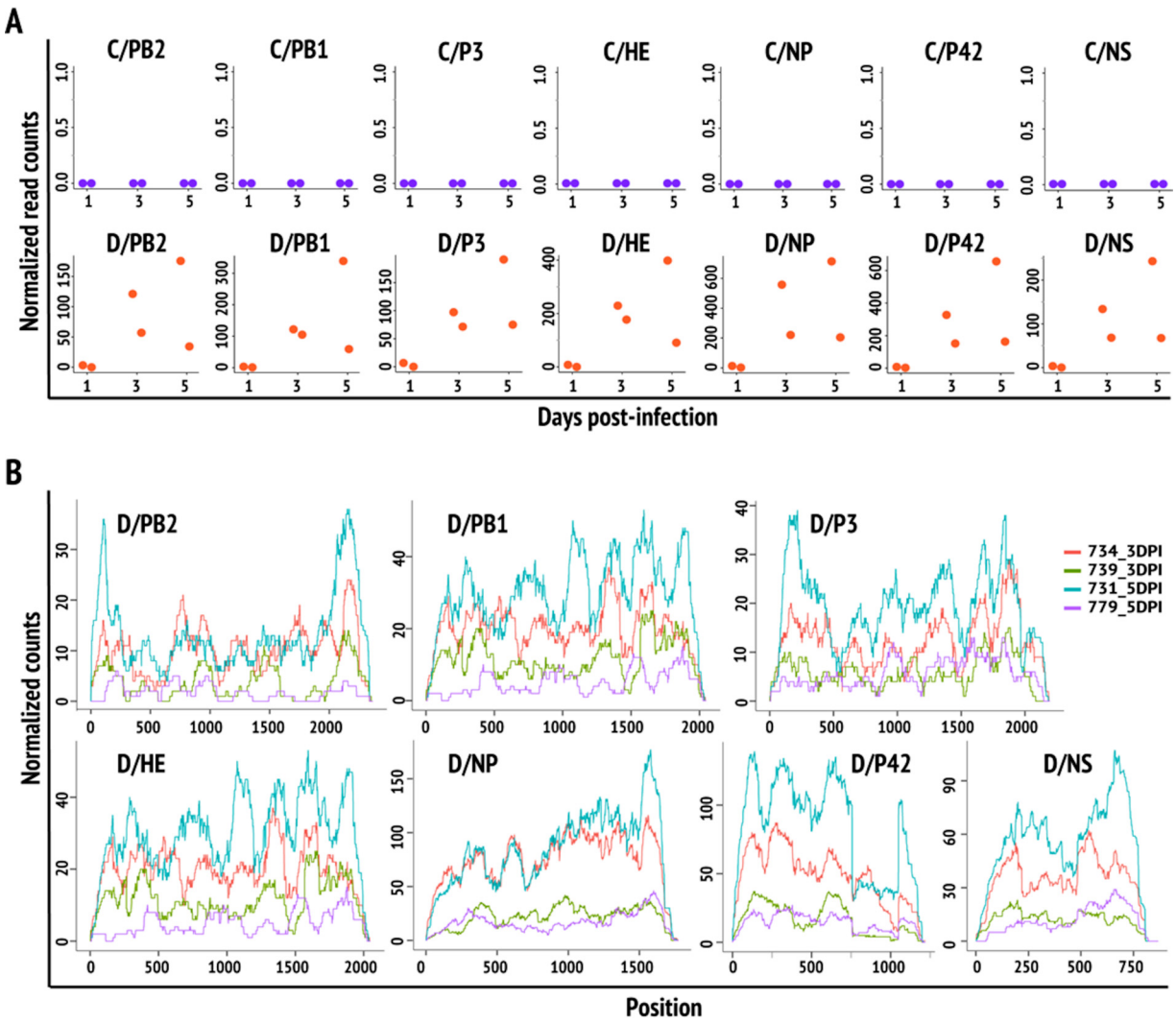

FIG 7 RNA-Seq analysis of lung viral transcriptomes of ICV and IDV. Next-generation sequencing analyses were conducted to characterize viral transcriptomes derived from the lungs of huICV and swIDV-infected guinea pigs. Numbers of normalized read counts for each gene segment plotted against the days postinfection were given for huICV and swIDV (A). Numbers of normalized sequence reads of swIDV mapped to each nucleotide position for each gene segment for the two sampled animals from 3 dpi and 5 dpi were given in (B).

inflammatory changes at 5 dpi (Fig. 8B). The representative images at 5 dpi are shown in Fig. 8. In swIDV infected lungs, there was severe interstitial pneumonia characterized by inflammatory cell infiltrations (3 and 5 dpi), peribronchial, and perivascular cuffing (blue arrow) by lymphocytes and plasma cells, and bronchopneumonia with luminal exudate observed on 3, 5, and 7 dpi (Fig. 9D1-D4). Compared to swIDV, the extent of inflammatory changes in the lung parenchyma was less in huICV-infected animals. Bronchiolar changes were shown in the insets of Fig. 9. In swIDV group, the bronchiolar epithelium suffered severe denudation (orange arrow) with exudate compared to the huICV-infected guinea pigs. The lungs from mock-infected animals did not show inflammatory cells or pneumonic changes (Fig. 9E).

Seroconversion. To check the seroconversion, two intranasally inoculated animals from each group were maintained until 14 dpi. Pre- and postinfection sera from all the animals in the huICV and swIDV groups (days 1, 3, 5, 7, 14 postinfection) and mock animals were tested for the presence of antibody against huICV and swIDV by microneutralization assay (Fig. 10A and B). All the animals were seronegative to both IDV and ICV before the intranasal virus inoculation. The individual MN titers for the animals in the huICV group at different time points were given in the parentheses:1 dpi (<10,<10),

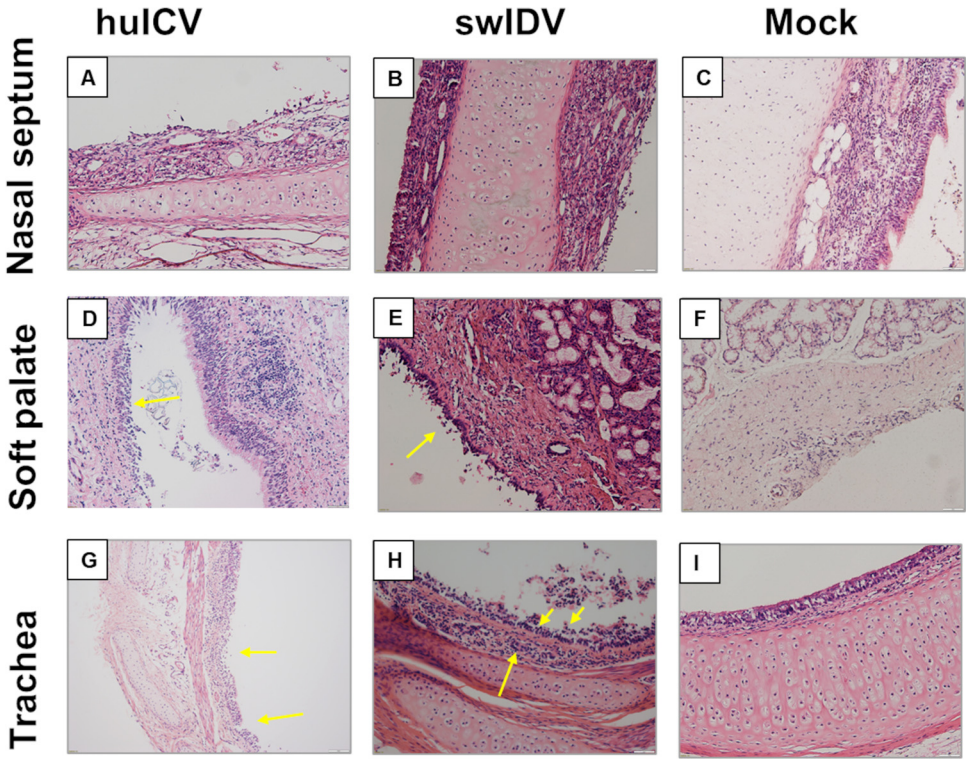

FIG 8 Histopathological changes in the nasal septum, soft palate, and trachea upon infection with huICV and swIDV in guinea pigs, compared to mock animals. Representative images of histopathological changes in the respiratory tract tissues on 5 dpi—Nasal septum with huICV (A), swIDV (B), and with mock (C); the soft palate with huICV (D), swIDV (E), and with mock (F); trachea with huICV (G), swIDV (H), and with mock (I). Histologically, the lining epithelium of the nasal mucosa showed minimal to mild inflammatory changes in both huICV and swIDV groups compared to mock-infected animals. Both soft palate and trachea lining epithelium suffered mild to moderate inflammatory changes with disruptive mucosal changes (yellow arrows), and lymphoplasmacytic infiltrations in the submucosa. Tissues from the mock animal on 7 dpi showed no such inflammatory changes.

3 dpi (<10,<10), 5 dpi (<10,<10), 7 dpi (<10,<10), 14 dpi (<10,80). In the case of swIDV, the individual MN titers were 1 dpi (<10,<10), 3 dpi (<10,<10), 5 dpi (<10,<10), 7 dpi (80, 160), and 14 dpi (1280, 1280). Compared to swIDV, the seroconversion occurred late at 14 dpi in the huICV group and only 1/2 guinea pigs showed a titer of 80. The other animal without detectable HI antibody titer never shed the virus on any day, indicating that an abortive infection might have happened in that animal. In the case of swIDV, antibody responses were detected in 2/2 animals as early as 7 dpi (80, 160) and reached a higher titer of 1280 by 14 dpi. Human ICV sera showed no cross-reactivity with swIDV (Fig. 10C). Similarly, sw IDV sera exhibited no cross-reactivity with huICV and also demonstrated a homologous high titer of 1280 (Fig. 10D).

DISCUSSION

Despite its ubiquitous nature and high seroprevalence in human adults, little is known about the differential pathogenesis and *in vivo* tropism of ICV compared to IAV and IBV. Besides, ICV has been isolated from dogs, pigs, and cattle indicating that this virus can jump species barriers and infect both agricultural and companion animals. Influenza C viruses are neglected despite the emerging evidence of the increasing clinical significance of ICV-associated CAP in children under 2 years old (35) and its rate of co-infection involving bacteria (*Haemophilus influenzae*) and viruses is much more common than that observed for IAV and IBV. There are no effective vaccines or antivirals available to treat huICV infection, although ICV can result in severe acute respiratory disease in infants/children (32, 83). Given the importance of these two seven-segmented viruses in the infection landscape of influenza, it would be very instrumental in studying the differential

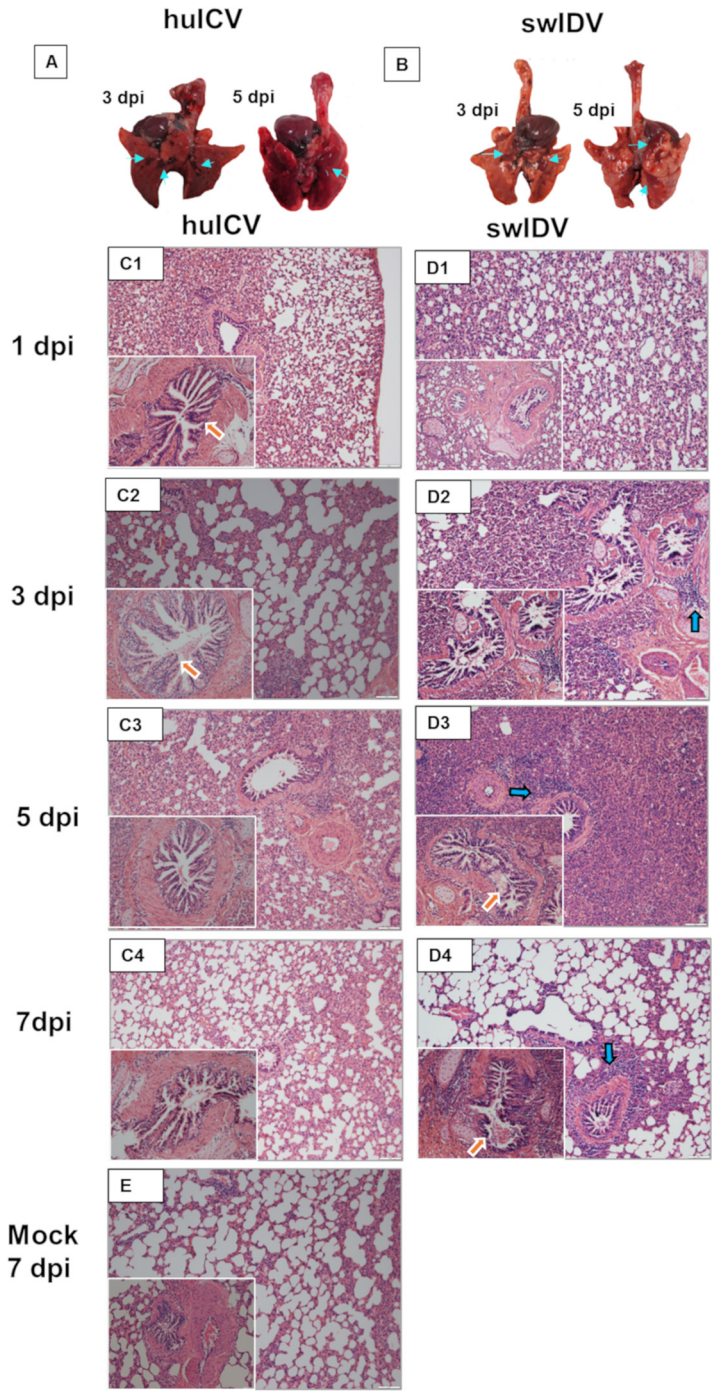

FIG 9 Pathological changes in lungs of guinea pigs infected with huICV and swIDV, compared to mock animals. Representative images of macroscopic lesions at 3 and 5 dpi of the lungs from huICV-infected animals are shown in A and that of swIDV are shown in B. Cyan arrows show areas of pulmonary consolidation. Representative images of histopathological lesions in the lungs were shown for animals on 1, 3, 5, and 7 dpi for huICV (C1, C2, C3, C4); swIDV (D1, D2, D3, D4) compared to the mock (E). Histologically, the lung tissue showed multifocal areas of alveolar inflammation with infiltration of lymphocytes, plasma cells (blue arrows), and RBCs in the lung parenchyma. Bronchiolar inflammation with desquamation of the epithelial cells and RBCs (orange arrows) and peribronchial infiltration of lymphocytes were also seen. Lungs from the mock animal on 7 dpi showed no such lesions.

pathogenesis and replication fitness of ICV and IDV that would provide a new effective avenue for assessing preventative and therapeutic measures.

Previous studies from our group and others have shown that ICV and IDV use *9-O*-acetylated sialic acids as a cellular receptor for virus entry and infection (69, 70).

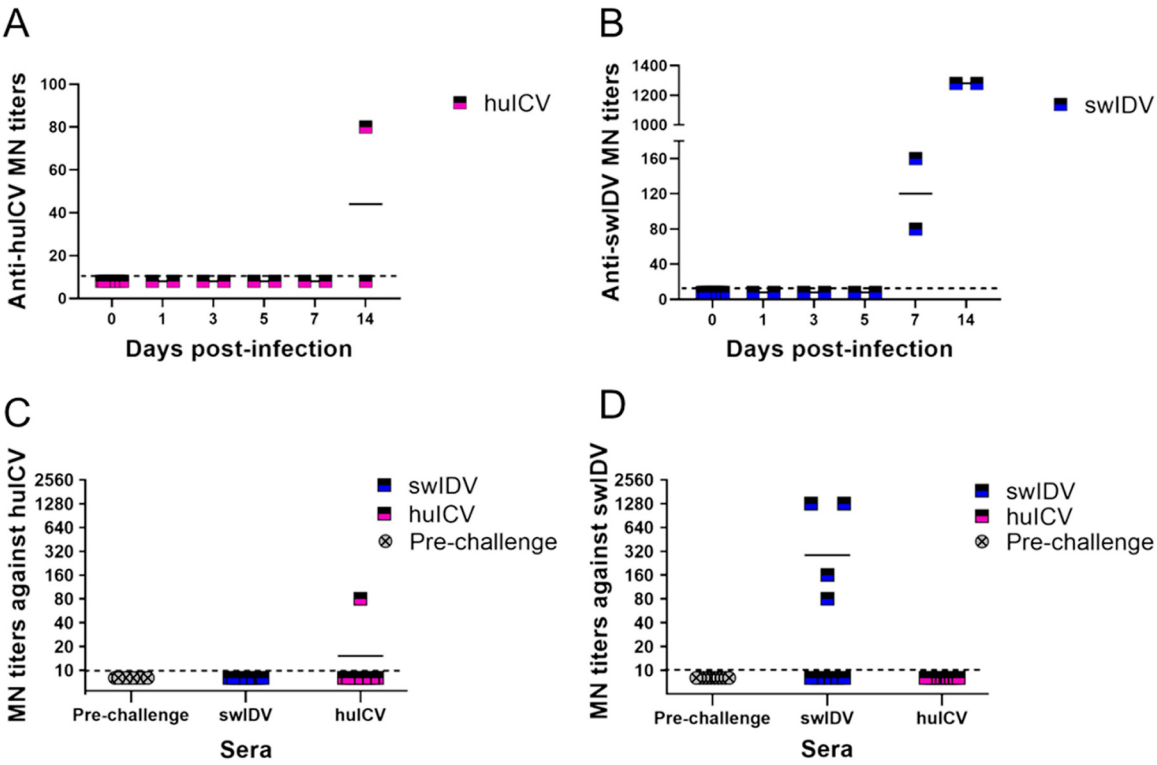

FIG 10 Guinea pigs seroconverted after infection with huICV and swIDV and the antibodies showed no evidence of cross-reactivity. Microneutralization (MN) assay was used to determine the antibody titer of the guinea pigs after infection with huICV and swIDV. The MN titers (Y axis) of the animals plotted individually against different time points (X axis) against huICV and swIDV are shown in A and B respectively. A dotted line indicating the limit of detection is also shown. Pre and postchallenge sera of all infected animals of both virus groups were also tested against both huICVand swIDV. Both ICV and IDV sera showed no evidence of cross-reactivity. The *x* axis represents the pre-challenge and postchallenge sera against viruses used in the study and *y* axis represents MN titers against (C) huICVand (D) swIDV. Each shape represents an individual animal and mean MN titers are shown.

Moreover, our previous work established that ICV-related IDV could replicate productively in the URT and LRT of the guinea pigs and also demonstrated direct contact transmission (74). As a first step, we analyzed the sialic acid receptor distribution in the respiratory tract of the guinea pig by HPLC and found that ICV and IDV receptors are present abundantly in both upper and lower respiratory tracts. The presence of *9-O*-acetylated sialic acids, particularly the Neu5,9Ac2 in the guinea pig respiratory tract, supported the use of the guinea pigs to study these two viruses (79, 80).

Guinea pigs have been used previously to study IDV replication and pathogenesis. To date, this animal model was not yet explored to study ICV infection. Host response variability of the guinea pigs could represent the genetic diversity of the susceptible human population which is an important determinant of outcomes and severity of illness associated with ICV infections in children. Here, we demonstrated that guinea pigs after intranasal inoculation of ICV did not show any clinical symptoms or changes in body weight or temperature, consistent with the clinical observations obtained from our previous study where guinea pigs were inoculated with bovine IDV (74). However, ICV-infected animals demonstrated nasal shedding and virus tissue tropism toward URT tissues such as nasal turbinate, and soft palate. It is generally believed that ICV is an upper respiratory pathogen in adult humans and normally lacks a lung tropic capacity (84). The results of our ICV tropism study in guinea pigs are overall consistent with this theory because multiple approaches used in our study collectively demonstrated that huICV strain replicated only in the nasal turbinate, and soft palate of the guinea pigs. In the case of the LRT tissues, an appreciable virus load was found in the trachea while neither active viral replication nor viral genome was detected in the lungs. The tracheal temperature of healthy human volunteers ranged from 31–32°C during inspiration and 33–36°C during expiration (85). Despite being part of LRT,

the temperature of the human tracheal airways is reported to be slightly lower than the core body temperature and depends on the ambient temperature and humidification (86), which could be a reason for the ICV replication in the trachea. Compared to swIDV, huICV failed to replicate in the lungs, which confirms the intrinsic temperature sensitivity of the ICV-hemagglutinin esterase fusion (HEF) protein at 37°C (91). Our *in vitro* replication kinetics study using species-specific cell lines from the dog, pig, and humans also demonstrated the limited ICV growth at 37°C, compared to 33°C (Fig. 1). The ICV replication kinetics and tropism in guinea pigs largely recapitulate what has been observed in humans where ICV replication is primarily confined to the upper, and not to the LRT. At 37°C, ICV HEF-mediated membrane fusion decreases due to the low efficiency of the membrane fusion pore formation. In addition, the core body temperature of 37°C could impair protein oligomerization which in turn affects the trimerization and transportation of the influenza C viral proteins from the endoplasmic reticulum to the plasma membrane via Golgi, subsequently leading to low HEF expression at the plasma membrane. We speculate that these factors could be the reason why huICV failed to replicate in the lungs (87). It should be noted that ICV infections in children generally cause URT infection but can be associated with lower respiratory tract infection in complicated cases of co-infections involving other microbial agents. ICV replication in the trachea of guinea pigs observed here appears to support this clinical observation. Further, deep RNA sequencing did not reveal any significant adaptive mutations. Analyses of the field strains of IDV and ICV available in the database revealed that the mutations observed in the ICV and IDV genome in the nasal washes compared to the inoculum genome sequence were random mutations and further studies are needed to understand whether these mutations have any biological relevance.

A comprehensive comparative evaluation of the pathogenetic mechanisms of ICV and IDV was carried out to determine the key differences and similarities in the viral replication, tissue tropism, and pathogenesis between these two distantly related viruses. Guinea pigs after inoculation of ICV and IDV exhibited several similar characteristics including no detectable virus shedding on 1 dpi, tropism to URT, and seroconversion. The pathology associated with ICV and IDV was similar and no significant differences in gross lesions were noted in the URT between the two groups. Histopathological changes in the respiratory epithelium of the soft palate and trachea were similar in both huICV and swIDV groups. However, lung lesions on 3 and 5 dpi were more pronounced in animals infected with swIDV than those with huICV, which shows the slow progression of ICV compared to IDV. Inflammatory changes observed in huICV- infected lungs, without any productive viral replication suggest the possibility of co-infections, which warrant further investigation. Considering 8-week-old guinea pigs correspond to the adolescent stage in humans (88, 89), the use of 5–6 weeks old ICV infected animals in our study approximate to 10 human years (as per World Health Organization, the age of adolescence ranges from 10–19 years) and the pathological correlates demonstrated by these guinea pigs agree with pathological changes found in an adolescent human, characterized by marked URT histopathological changes than LRT. Guinea pig co-infection models of ICV are needed in the future to investigate the co-infection dynamics of ICV.

Significantly, several key differences were observed between ICV and IDV groups as summarized below. First, the IDV group demonstrated a more uniform and accelerated rate of virus shedding following infection when compared to the ICV group. Second, despite no detectable virus shedding in nasal washes on 1 dpi, there was a high virus titer in the swIDV group on 3 dpi and 5 dpi compared to the huICV group. Third, viral loads of swIDV in the soft palate peaked at 3 dpi with no appreciable titer at 7 dpi, whereas in huICV animals, viral load was present at 5 and 7 dpi, even though there were no appreciable titers on 1 and 3 dpi. Fourth, huICV did not show tropism to LRT tissues such as lungs as confirmed by both ISH and next-generation sequencing approaches. We speculate that the key differences in the viral replication patterns demonstrated by the huICV and swIDV could be attributed to the differences in the receptor-binding domain of the HEF protein or due to any other viral genetic factors. Also, the broad cell tropism exhibited by the IDV may be attributed to the open

receptor-binding cavity of the hemagglutinin-esterase fusion glycoprotein that can accommodate diverse glycan moieties and better receptor binding affinity (69). Lastly, a shorter seroconversion period and more uniform antibody kinetics was observed in swIDV compared to huICV group. A previous study using D/660 lineage virus in guinea pigs also demonstrated similar research outcomes such as active replication in the upper and lower respiratory tract, presence of contact transmission, and seroconversion in direct inoculated animals (74).

Interestingly, experimental infections in dogs where the animals were exposed three times to C/Ann Arbor/1/50, also showed variations in the severity of the infection with virus isolation reported only in 4/6 dogs after the second inoculation and the time taken for seroconversion varied considerably between animals (90). A non-uniform and recurring trend of virus excretion were also observed in experimental infection of ICV in pigs where the directly inoculated pigs showed intermittent virus excretion and contact transmission (57). Pigs infected with C/pig/Beijing/32/81 showed antibody responses in all six animals which included both direct inoculated and contacted animals, whereas pigs infected with human ICV strain C/NJ/1/76 showed seroconversion in only 2/6 animals which indicate the variability in antibody response between ICVs of different species origin (57). The C/Victoria/2/2012 strain we used for this study has not been studied *in vivo*. Experimental studies with longer periods of disease monitoring and viral shedding using ICVs of different host species origins will help to understand more about the species-specific virulence and tissue tropism of the influenza C viruses.

In summary, the results of our experiments provided encouraging evidence that guinea pigs can be used as a suitable small animal model, to study the replication fitness and tissue tropism of both ICV and IDV without the need for prior adaptation. The lack of uniform response by all ICV-infected animals is a limitation of our study, which could be due to the age/strain of the guinea pig, virus strain used, the dose of the inoculum, and other variables. However, the ICV tissue tropism was uniformly evident in the URT of the guinea pigs. The results of this comparative animal model study shall help us to understand the differences in replication fitness and tissue tropism between ICV and IDV. The findings we observed for ICV in guinea pigs could be of great value for further exploring this species as an animal model in the future for the evaluation of potential vaccines or antiviral compounds against influenza C virus, a potential, yet, underrecognized respiratory pathogen of children.

MATERIALS AND METHODS

Cells, viruses, and Animals. The swIDV used for intranasal inoculation was grown on human rectal carcinoma (HRT-18G) cells and huICV was grown on Madin Darby Canine Kidney (MDCK) cells. The viruses/samples from the animals were titrated with the $TCID_{50}$ readout on MDCK cells by making serial 10-fold dilutions of the samples in DMEM supplemented with 1 μg/mL tosylsulfonyl phenylalanyl chloromethyl ketone (TPCK)-trypsin and 1% antibiotic-antimycotic. Further, the viral stocks were sequenced by the *Illumina* MiSeq (see the below for the detailed procedure). Specific-pathogen-free (SPF), influenza D virus-specific antibody-free (SPF/VAF), 30-day-old guinea pigs of the Dunkin-Hartley strain (Elm Hill Labs, MA, USA) weighing 300 to 350 g were used for the study. The animals were ear-tagged for identification purposes. The duration of the experiment was 3 weeks, which included a 1-week acclimatization period. Animals were provided with food and water *ad libitum* and kept on a 12-h light/dark cycle. The temperature and relative humidity (RH) of the animal housing ranged from 72°F to 75°F and 25% to 33%, respectively. Control animals were housed in a separate room away from the room housing the infected animals and were processed before the inoculated animals. Strict precautionary measures were followed to prevent cross-contamination between animals in different cages. Gloves were changed between cages during cleaning and handling, and masks and surfaces were disinfected to prevent any possible cross-contamination.

Experimental design. Guinea pigs were divided into experimental groups for testing the growth kinetics of the virus. Two virus-infected groups included (1) influenza D/swine/Oklahoma/1334/2011, and (2) C/Victoria/2/2012. The group for studying virus kinetics consisted of 10 infected animals and 5 mock-infected animals. The animals were infected intranasally with 3×10^5 50% tissue culture infective doses. Half (150 μL) of the virus inoculum was delivered in each nostril. The 5 control animals were mock infected with equal volumes of phosphate-buffered saline (PBS). The body weights of all the animals were recorded before the challenge and days after the challenge. Guinea pigs were briefly anesthetized using isoflurane before infection. The animal experiments were approved by the Institutional Animal Care and Use Committee of South Dakota State University (IACUC no. 15-017A) and were conducted under biosafety level 2 conditions at the Animal Research Wing of South Dakota State University.

Monitoring and sample collection. Bodyweight and temperature were monitored daily starting 2 days before the challenge. Prior to the challenge, blood was collected from all the animals from the jugular vein/cranial vena cava under conditions of isoflurane anesthesia. Animals were monitored daily after the virus challenge for clinical signs, and body temperature and body weight were recorded. Nasal washes were collected from all the infected animals in the directly inoculated group and from three control animals at 1, 3, 5, and 7, days postinfection (dpi). Additionally, two infected animals were euthanized using CO_2 at 1, 3, 5, and 7 dpi. Blood, nasal wash, nasal turbinate, soft palate, trachea, and lung samples were collected. The numbers of infected animals assessed each day from group I were as follows: day 1, $n = 10$; days 2 and 3, $n = 8$; days 4 and 5, $n = 6$; days 6 and 7, $n = 4$; days 8–14, $n = 2$. Two animals from each group were kept for antibody development toward seroconversion. These animals were euthanized at 14 dpi, and blood, nasal wash, nasal turbinate, soft palate, trachea, and lung samples were collected.

Collection of nasal washes. The nasal washes were collected by instilling 1 mL of PBS using a sterile 25-to-28-gauge cannula into the nostrils and collecting the washes by draining them into sterile containers or Petri dishes. Animals were anesthetized using isoflurane, and alternate nostrils were used for sample collection on alternate days. Nasal washes collected in the Petri dishes were transferred to 1.5-mL tubes and then centrifuged at 500 $\times$ *g* for 6 min at 4°C to remove any debris. The supernatants were stored at −80°C until further analysis.

Estimation of virus load in nasal washes and tissues. Nasal turbinates, soft palate, trachea, and lung, from guinea pigs were collected and stored at −80°C. One gram of tissue was homogenized using DMEM supplemented with penicillin-streptomycin (Life Technologies, Carlsbad, CA, USA) (200 U/mL) and a Stomacher circulator at high speed for 2 min. The homogenized tissue fluid was clarified by spinning at 500 $\times$ *g* for 8 min at 4°C and stored at −80°C. For trachea and nasal turbinate analyses, DMEM with penicillin-streptomycin (Life Technologies, Carlsbad, CA, USA) (200 U/mL) was added and homogenized tissue fluid was collected and stored at −80°C until titration.

For virus isolation, MDCK cells were used for determining the virus titer present in nasal washes and tissue homogenates. 7×10^3 cells were seeded on 96-well tissue culture plates and allowed to grow overnight. When the cells reached 60–70% confluent, serial 10-fold dilutions of the sample were inoculated on cell culture plates after the plates were washed with sterile PBS. The inoculated cell culture plates were incubated for 5 days at 37°C. After 5 days, hemagglutination was carried out on the infected cell culture plates using 1% turkey RBCs, for the determination of virus titer in nasal washes and tissues. Virus titration was determined using the Reed and Muench formula to find the 50 percent endpoints (77).

RNA Sequencing. All the RNA samples were quality checked with Bioanalyzer RNA 6000 nano kit, using Eukaryotes total RNA assay with RNA integrity number (RIN) over 7. The poly-A mRNA was purified from total RNA using the oligo (dT) magnetic beads, and library preparation was performed using TruSeq stranded mRNA library Prep kit (catalog ID: 20020595, Illumina Inc). These short mRNA fragments were used as templates for first-strand cDNA synthesis by reverse transcriptase SuperScript II (catalog ID:18064014, ThermoFisher) using random hexamer primers. The RNA template was removed, and a replacement strand was synthesized to generate ds cDNA during the 2nd strand synthesis. These ds cDNA fragments were purified using AMPure XP beads followed by A-tailing and adapter ligation with index kit (catalog ID: 20020492, 2002049, Illumina Inc). The ligation reaction products were enriched by PCR (PCR) for 15 cycles, and the products were purified by AMPure beads to create the final cDNA library. The PCR-enriched library was quantified with Qubit HS dsDNA and the library peaks were examined with Bioanalyzer DNA nano kit. A final diluted 1.3 mL of 1.8pM of the pooled library was sequenced from 2 runs of single end using NextSeq 500 sequencing platform with High Output 150 cycles (catalog ID: TG-160-2002, Illumina, Inc).

RNA-Seq data analysis. We first excluded low-quality RNA-Seq raw reads (Qscore $<$20). To reduce the effect of PCR amplification on expression level quantification, we removed PCR duplicates using FastUniq version 1.1 (91). The reference influenza C and D genomes were downloaded from the Influenza Research Database (IRD, https://www.fludb.org/brc/home.spg?decorator=influenza) (92). The remaining unique reads were mapped to ICV, IDV, and guinea pig genomes (Cavpor3.0, Ensembl release 89) using Bowtie2 (93). To calculate the expression levels of both viral and host genes in each sample, we first calculated the numbers of reads mapped to each gene using HTSeq version 0.9.1, with reads mapped to multiple genes counted for each gene (94). We then used DESeq2 to normalize gene expression levels (95). Positional gene expression was calculated using Samtools (96).

Microneutralization (MN)Assay. The pre- and postinfection sera were treated with the receptor-destroying enzyme (Denka Seiken, Chuo-ku, Tokyo, Japan) before conducting the MN assay. RDE treatment was done according to the manufacturer's protocol and MN assay was performed as described previously (9, 10, 97). After incubation period, the titers were estimated by performing hemagglutination assay using 1% turkey RBCs (Lampire Biological Laboratories, Pipersville, PA, USA).

Histopathology and *in-situ* hybridization. Following the experimental infection of guinea pigs, euthanasia was performed at prescribed time points. A complete necropsy was performed to examine any macroscopic lesion in all the organs. Nasal turbinate, soft palate, trachea, and lung samples were collected in 10% neutral buffered formalin and embedded in paraffin wax. Sections (5 μm thick) were then cut and stained with hematoxylin and eosin for histopathological examination. IDV in respiratory tract tissues was detected using *in situ* hybridization (ISH) with radioactive isotopes of sulfur (^{35}S) labeled negative-sense RNA probes of nucleoprotein (NP) as described previously (71).

High-performance liquid chromatography. Whole samples were frozen with liquid nitrogen before homogenization with mortar and pestle, then reconstituted at a concentration of ~8g per 25 mL in a 50 mM sodium maleate solution at pH 6.5 containing sucrose at a concentration of 0.5 M. The

solutions were ultra-centrifuged at 650 × *g* for 10 min, the supernatant was collected while the pellet was resuspended before the second round of ultracentrifugation. All supernatant fractions were combined to form the total post-nuclear supernatant. Diisopropyl fluorophosphate (DFP) was added at 1 mM concentration and the sample was incubated on ice for 30 min. the samples were then diluted 1:20 with ice-cold water, EDTA was added at a concentration of 1 mM, the sample was further ultra-centrifuged at 1,00,000 × *g* for 30 min. The supernatant was removed and discarded, the pellet was resuspended in 1 M NaCl and spun again for 30 min. The supernatant was again removed from the clean pellet, and the pellet was resuspended in 50 mM Tris-HCl, pH 6.5. Approximately 1:10 of the total isolated membrane sample was taken for sialic acid analysis. Sialic acids were released enzymatically and separated from the proteins by passing the sample through a C18 SPE cartridge. The sialic acid fraction was then dried and concentrated via SpeedVac. Released sialic acids were labeled through reductive animation with DNB in a reaction solution of acetic acid and B-mercaptoethanol in a screw-top vial for 2h at 55°C. The reaction was halted by snap-freezing, before dilution of the sample with 100X water. Labeled sialic acids were separated via C18 separation (Supelco C18) attached to an Agilent 1200 Infinity HPLC system equipped with a Fluorescence Detector. The excitation and emission of wavelengths were 373 nm and 448 nm respectively. One microliter of the sample was injected, and the separation conditions were an isocratic elution of 9:7:84 ACN: MeOH: H2O at 0.4 mL/min for 20 min. A standard curve of different sialic acids was also separated for identification.

ACKNOWLEDGMENTS

This study was supported by NIH R01AI141889, SDSU-AES 3AH-673, National Science Foundation/EPSCoR (http://www.nsf.gov/od/iia/programs/epscor/index.jsp) award IIA-1335423, and the SD-CBRC supported by the State of South Dakota's Governor's Office of Economic Development. The authors also thank the support provided by the William Robert Mills Chair Endowment Fund and Agricultural Experiment Station of the University of Kentucky. Besides, We thank the animal research wing of South Dakota State University for their assistance and support in conducting the guinea pig study and CRCC, the University of Georgia for their help in quantitative measurement of sialic acid receptors in tissues of guinea pigs. We also thank Dr. Angela Pillatzki and Amanda Brock (Animal Disease diagnostic and research lab, South Dakota State University) for their assistance in Histology; Mike Hildreth (Functional Genomics Core facility, South Dakota State University for providing help with the imaging). The members of the Wang-Li lab are particularly appreciated for their great help in animal experiments described in this manuscript.

REFERENCES

1. Anonymous. 2018. Orthomyxoviridae, Virus Taxonomy: 2018b Release.
2. Elliott RM, Yuanji G, Desselberger U. 1985. Protein and nucleic acid analyses of influenza C viruses isolated from pigs and man. Vaccine 3:182–188. https://doi.org/10.1016/0264-410x(85)90100-8.
3. Buonagurio DA, Nakada S, Fitch WM, Palese P. 1986. Epidemiology of influenza C virus in man: multiple evolutionary lineages and low rate of change. Virology 153:12–21. https://doi.org/10.1016/0042-6822(86)90003-6.
4. Buonagurio DA, Nakada S, Desselberger U, Krystal M, Palese P. 1985. Noncumulative sequence changes in the hemagglutinin genes of influenza C virus isolates. Virology 146:221–232. https://doi.org/10.1016/0042-6822(85)90006-6.
5. Matsuzaki Y, Sugawara K, Furuse Y, Shimotai Y, Hongo S, Oshitani H, Mizuta K, Nishimura H. 2016. Genetic Lineage and Reassortment of Influenza C Viruses Circulating between 1947 and 2014. J Virol 90:8251–8265. https://doi.org/10.1128/JVI.00969-16.
6. Yu J, Li F, Wang D. 2021. The first decade of research advances in influenza D virus. J Gen Virol 102. https://doi.org/10.1099/jgv.0.001529.
7. Hause BM, Ducatez M, Collin EA, Ran Z, Liu R, Sheng Z, Armien A, Kaplan B, Chakravarty S, Hoppe AD, Webby RJ, Simonson RR, Li F. 2013. Isolation of a novel swine influenza virus from Oklahoma in 2011 which is distantly related to human influenza C viruses. PLoS Pathog 9:e1003176. https://doi.org/10.1371/journal.ppat.1003176.
8. Hause BM, Collin EA, Liu R, Huang B, Sheng Z, Lu W, Wang D, Nelson EA, Li F. 2014. Characterization of a novel influenza virus in cattle and Swine: proposal for a new genus in the Orthomyxoviridae family. mBio 5:e00031-14–e00014. https://doi.org/10.1128/mBio.00031-14.
9. Nedland H, Wollman J, Sreenivasan C, Quast M, Singrey A, Fawcett L, Christopher-Hennings J, Nelson E, Kaushik RS, Wang D, Li F. 2018. Serological evidence for the co-circulation of two lineages of influenza D viruses in equine populations of the Midwest United States. Zoonoses Public Health 65:e148–e154. https://doi.org/10.1111/zph.12423.
10. Quast M, Sreenivasan C, Sexton G, Nedland H, Singrey A, Fawcett L, Miller G, Lauer D, Voss S, Pollock S, Cunha CW, Christopher-Hennings J, Nelson E, Li F. 2015. Serological evidence for the presence of influenza D virus in small ruminants. Vet Microbiol 180:281–285. https://doi.org/10.1016/j.vetmic.2015.09.005.
11. Alvarez IJ, Fort M, Pasucci J, Moreno F, Gimenez H, Näslund K, Hägglund S, Zohari S, Valarcher JF. 2020. Seroprevalence of influenza D virus in bulls in Argentina. J Vet Diagn Invest 32:585–588. https://doi.org/10.1177/1040638720934056.
12. Salem E, Cook EAJ, Lbacha HA, Oliva J, Awoume F, Aplogan GL, Hymann EC, Muloi D, Deem SL, Alali S, Zouagui Z, Fevre EM, Meyer G, Ducatez MF. 2017. Serologic Evidence for Influenza C and D Virus among Ruminants and Camelids, Africa, 1991–2015. Emerg Infect Dis 23:1556–1559. https://doi.org/10.3201/eid2309.170342.
13. Chu DKW, Perera R, Ali A, Oladipo JO, Mamo G, So RTY, Zhou Z, Chor YY, Chan CK, Belay D, Tayachew A, Mengesha M, Regassa F, Lam NT, Poon LLM, Peiris M. 2020. Influenza A Virus Infections in Dromedary Camels, Nigeria and Ethiopia, 2015–2017. Emerg Infect Dis 26:173–176. https://doi.org/10.3201/eid2601.191165.
14. Murakami S, Odagiri T, Melaku SK, Bazartseren B, Ishida H, Takenaka-Uema A, Muraki Y, Sentsui H, Horimoto T. 2019. Influenza D Virus Infection in Dromedary Camels, Ethiopia. Emerg Infect Dis 25:1224–1226. https://doi.org/10.3201/eid2506.181158.
15. Flynn O, Gallagher C, Mooney J, Irvine C, Ducatez M, Hause B, McGrath G, Ryan E. 2018. Influenza D Virus in Cattle, Ireland. Emerg Infect Dis 24:389–391. https://doi.org/10.3201/eid2402.170759.
16. White SK, Ma W, McDaniel CJ, Gray GC, Lednicky JA. 2016. Serologic evidence of exposure to influenza D virus among persons with occupational contact with cattle. J Clin Virol 81:31–33. https://doi.org/10.1016/j.jcv.2016.05.017.

17. Trombetta CM, Montomoli E, Di Bartolo I, Ostanello F, Chiapponi C, Marchi S. 2022. Detection of antibodies against influenza D virus in swine veterinarians in Italy in 2004. J Med Virol 94:2855–2859. https://doi.org/10.1002/jmv.27466.
18. Trombetta CM, Marchi S, Manini I, Kistner O, Li F, Piu P, Manenti A, Biuso F, Sreenivasan C, Druce J, Montomoli E. 2019. Influenza D Virus: Serological Evidence in the Italian Population from 2005 to 2017. Viruses 12:30. https://doi.org/10.3390/v12010030.
19. Bailey ES, Fieldhouse JK, Alarja NA, Chen DD, Kovalik ME, Zemke JN, Choi JY, Borkenhagen LK, Toh TH, Lee JSY, Chong KS, Gray GC. 2020. First sequence of influenza D virus identified in poultry farm bioaerosols in Sarawak, Malaysia. Trop Dis Travel Med Vaccines 6:5. https://doi.org/10.1186/s40794-020-0105-9.
20. Bui VN, Nguyen TT, Nguyen-Viet H, Bui AN, McCallion KA, Lee HS, Than ST, Coleman KK, Gray GC. 2019. Bioaerosol Sampling to Detect Avian Influenza Virus in Hanoi's Largest Live Poultry Market. Clin Infect Dis 68:972–975. https://doi.org/10.1093/cid/ciy583.
21. Kawamura H, Tashiro M, Kitame F, Homma M, Nakamura K. 1986. Genetic variation among human strains of influenza C virus isolated in Japan. Virus Res 4:275–288. https://doi.org/10.1016/0168-1702(86)90006-7.
22. Darke CS, Watkins PH, Whitehead JE. 1957. Fulminating staphylococcal pneumonia associated with influenza virus C: report of a fatal case. Br Med J 2:606–609. https://doi.org/10.1136/bmj.2.5045.606.
23. Taylor RM. 1949. Studies on survival of influenza virus between epidemics and antigenic variants of the virus. Am J Public Health Nations Health 39:171–178. https://doi.org/10.2105/ajph.39.2.171.
24. Hilleman MR, Werner JH, Gauld RL. 1953. Influenza antibodies in the population of the USA; an epidemiological investigation. Bull World Health Organ 8:613–631.
25. Yano T, Maeda C, Akachi S, Matsuno Y, Yamadera M, Kobayashi T, Nagai Y, Iwade Y, Kusuhara H, Katayama M, Fukuta M, Nakagawa Y, Naraya S, Takahashi H, Hiraoka M, Yamauchi A, Nishinaka T, Amano H, Yamaguchi T, Ochiai H, Ihara T, Matsuzaki Y. 2014. Phylogenetic analysis and seroprevalence of influenza C virus in Mie Prefecture, Japan in 2012. Jpn J Infect Dis 67:127–131. https://doi.org/10.7883/yoken.67.127.
26. Moriuchi H, Katsushima N, Nishimura H, Nakamura K, Numazaki Y. 1991. Community-acquired influenza C virus infection in children. J Pediatr 118:235–238. https://doi.org/10.1016/s0022-3476(05)80489-5.
27. Hirsila M, Kauppila J, Tuomaala K, Grekula B, Puhakka T, Ruuskanen O, Ziegler T. 2001. Detection by reverse transcription-polymerase chain reaction of influenza C in nasopharyngeal secretions of adults with a common cold. J Infect Dis 183:1269–1272. https://doi.org/10.1086/319675.
28. Calvo C, Garcia-Garcia ML, Centeno M, Perez-Brena P, Casas I. 2006. Influenza C virus infection in children, Spain. Emerg Infect Dis 12:1621–1622. https://doi.org/10.3201/eid1210.051170.
29. Matsuzaki Y, Abiko C, Mizuta K, Sugawara K, Takashita E, Muraki Y, Suzuki H, Mikawa M, Shimada S, Sato K, Kuzuya M, Takao S, Wakatsuki K, Itagaki T, Hongo S, Nishimura H. 2007. A nationwide epidemic of influenza C virus infection in Japan in 2004. J Clin Microbiol 45:783–788. https://doi.org/10.1128/JCM.01555-06.
30. Anton A, Marcos MA, Codoner FM, de Molina P, Martinez A, Cardenosa N, Godoy P, Torner N, Martinez MJ, Ramon S, Tudo G, Isanta R, Gonzalo V, de Anta MT, Pumarola T. 2011. Influenza C virus surveillance during the first influenza A (H1N1) 2009 pandemic wave in Catalonia, Spain. Diagn Microbiol Infect Dis 69:419–427. https://doi.org/10.1016/j.diagmicrobio.2010.11.006.
31. Matsuzaki Y, Ikeda T, Abiko C, Aoki Y, Mizuta K, Shimotai Y, Sugawara K, Hongo S. 2012. Detection and quantification of influenza C virus in pediatric respiratory specimens by real-time PCR and comparison with infectious viral counts. J Clin Virol 54:130–134. https://doi.org/10.1016/j.jcv.2012.02.012.
32. Njouom R, Monamele GC, Ermetal B, Tchatchouang S, Moyo-Tetang S, McCauley JW, Daniels RS. 2019. Detection of Influenza C Virus Infection among Hospitalized Patients, Cameroon. Emerg Infect Dis 25:607–609. https://doi.org/10.3201/eid2503.181213.
33. Lee HS, Lim S, Noh JY, Song JY, Cheong HJ, Lee JH, Woo SI, Kim WJ. 2019. Identification of influenza C virus in young South Korean children, from October 2013 to September 2016. J Clin Virol 115:47–52. https://doi.org/10.1016/j.jcv.2019.03.016.
34. Fritsch A, Schweiger B, Biere B. 2019. Influenza C virus in pre-school children with respiratory infections: retrospective analysis of data from the national influenza surveillance system in Germany, 2012 to 2014. Euro Surveill 24. https://doi.org/10.2807/1560-7917.ES.2019.24.10.1800174.
35. Thielen BK, Friedlander H, Bistodeau S, Shu B, Lynch B, Martin K, Bye E, Como-Sabetti K, Boxrud D, Strain AK, Chaves SS, Steffens A, Fowlkes AL, Lindstrom S, Lynfield R. 2018. Detection of Influenza C Viruses Among Outpatients and Patients Hospitalized for Severe Acute Respiratory Infection, Minnesota, 2013–2016. Clin Infect Dis 66:1092–1098. https://doi.org/10.1093/cid/cix931.
36. Potdar VA, Hinge DD, Dakhave MR, Manchanda A, Jadhav N, Kulkarni PB, Chadha MS. 2017. Molecular detection and characterization of Influenza 'C' viruses from western India. Infect Genet Evol 54:466–477. https://doi.org/10.1016/j.meegid.2017.08.005.
37. Ting PJ, Seah SG, Lim EA, Liaw JC, Boon-Huan T. 2016. Genetic characterisation of influenza C viruses detected in Singapore in 2006. Influenza Other Respir Viruses 10:27–33. https://doi.org/10.1111/irv.12352.
38. Smith DB, Gaunt ER, Digard P, Templeton K, Simmonds P. 2016. Detection of influenza C virus but not influenza D virus in Scottish respiratory samples. J Clin Virol 74:50–53. https://doi.org/10.1016/j.jcv.2015.11.036.
39. Giamberardin HI, Homsani S, Bricks LF, Pacheco AP, Guedes M, Debur MC, Raboni SM. 2016. Clinical and epidemiological features of respiratory virus infections in preschool children over two consecutive influenza seasons in southern Brazil. J Med Virol 88:1325–1333. https://doi.org/10.1002/jmv.24477.
40. Shimizu Y, Abiko C, Ikeda T, Mizuta K, Matsuzaki Y. 2015. Influenza C Virus and Human Metapneumovirus Infections in Hospitalized Children With Lower Respiratory Tract Illness. Pediatr Infect Dis J 34:1273–1275. https://doi.org/10.1097/INF.0000000000000863.
41. Kauppila J, Ronkko E, Juvonen R, Saukkoriipi A, Saikku P, Bloigu A, Vainio O, Ziegler T. 2014. Influenza C virus infection in military recruits–symptoms and clinical manifestation. J Med Virol 86:879–885. https://doi.org/10.1002/jmv.23756.
42. Jennings R. 1968. RESPIRATORY VIRUSES IN JAMAICA: A VIROLOGIC AND SEROLOGIC STUDY: 3. HEMAGGLUTINATION-INHIBITING ANTIBODIES TO TYPE B AND C INFLUENZA VIRUSES IN THE SERA OF JAMAICANS1. Am J Epidemiol 87:440–446. https://doi.org/10.1093/oxfordjournals.aje.a120834.
43. Minuse E, Davenport FM. 1951. Simultaneous recovery of type A' and type C influenza viruses from a patient. J Lab Clin Med 38:747–750.
44. Gerth HJ, Bauer KH, Steinitz H. 1975. Is there evidence for antigenic drift of influenza C viruses? (author's transl)]. Zentralbl Bakteriol Orig A 231:47–56.
45. O'Callaghan RJ, Gohd RS, Labat DD. 1980. Human antibody to influenza C virus: its age-related distribution and distinction from receptor analogs. Infect Immun 30:500–505. https://doi.org/10.1128/iai.30.2.500-505.1980.
46. Nishimura H, Sugawara K, Kitame F, Nakamura K, Sasaki H. 1987. Prevalence of the antibody to influenza C virus in a northern Luzon Highland Village, Philippines. Microbiol Immunol 31:1137–1143. https://doi.org/10.1111/j.1348-0421.1987.tb01348.x.
47. El-Rai FM, Shaheen YA, El-Diwani KM, Abdel-Al MH, Imam IZ, Hosny AH, El-Senousy AA. 1977. The incidence of antibodies to influenza C virus in Egyptian sera. J Egypt Public Health Assoc 52:6–11.
48. Tůmová B, Scharfenorth H, Adamczyk G. 1983. Incidence of influenza C virus in Czechoslovakia and German Democratic Republic. Acta Virol 27:502–510.
49. Govorkova EA, Zakstel'skaia L, Demidova SA. 1984. Detection of influenza virus C antibodies in the gamma globulins and native sera of children. Vopr Virusol 29:420–423.
50. Manuguerra JC, Hannoun C, Aymard M. 1992. Influenza C virus infection in France. J Infect 24:91–99. https://doi.org/10.1016/0163-4453(92)91150-a.
51. Manuguerra JC, Hannoun C, Sáenz MdC, Villar E, Cabezas JA. 1994. Seroepidemiological survey of influenza C virus infection in Spain. Eur J Epidemiol 10:91–94. https://doi.org/10.1007/BF01717459.
52. Suzuki T, Kondo M, Oda K, Takamiya A. 1987. [Epidemiological studies on type C influenza virus infection in Yokosuka city]. Kansenshogaku Zasshi 61:126–133. https://doi.org/10.11150/kansenshogakuzasshi1970.61.126.
53. Dykes AC, Cherry JD, Nolan CE. 1980. A clinical, epidemiologic, serologic, and virologic study of influenza C virus infection. Arch Intern Med 140:1295–1298. https://doi.org/10.1001/archinte.1980.00330210043021.
54. Zhang W, Zhang L, He W, Zhang X, Wen B, Wang C, Xu Q, Li G, Zhou J, Veit M, Su S. 2019. Genetic Evolution and Molecular Selection of the HE Gene of Influenza C Virus. Viruses 11:167. https://doi.org/10.3390/v11020167.
55. Zhang H, Porter EP, Lohman M, Lu N, Peddireddi L, Hanzlicek G, Marthaler D, Liu X, Bai J. 2018. Complete Genome Sequence of an Influenza C Virus Strain Identified from a Sick Calf in the United States. Microbiol Resour Announc 7. https://doi.org/10.1128/MRA.00828-18.
56. Zhang H, Porter E, Lohman M, Lu N, Peddireddi L, Hanzlicek G, Marthaler D, Liu X, Bai J. 2018. Influenza C Virus in Cattle with Respiratory Disease, United States, 2016–2018. Emerg Infect Dis 24:1926–1929. https://doi.org/10.3201/eid2410.180589.
57. Guo YJ, Jin FG, Wang P, Wang M, Zhu JM. 1983. Isolation of influenza C virus from pigs and experimental infection of pigs with influenza C virus. J Gen Virol 64 (Pt 1):177–182.

58. Manuguerra JC, Hannoun C. 1992. Natural infection of dogs by influenza C virus. Res Virol 143:199–204. https://doi.org/10.1016/s0923-2516(06)80104-4.
59. Manuguerra JC, Hannoun C, Simon F, Villar E, Cabezas JA. 1993. Natural infection of dogs by influenza C virus: a serological survey in Spain. New Microbiol 16:367–371.
60. Ohwada K, Kitame F, Sugawara K, Nishimura H, Homma M, Nakamura K. 1987. Distribution of the antibody to influenza C virus in dogs and pigs in Yamagata Prefecture, Japan. Microbiol Immunol 31:1173–1180. https://doi.org/10.1111/j.1348-0421.1987.tb01351.x.
61. Yamaoka M, Hotta H, Itoh M, Homma M. 1991. Prevalence of antibody to influenza C virus among pigs in Hyogo Prefecture, Japan. J Gen Virol 72:711–714. https://doi.org/10.1099/0022-1317-72-3-711.
62. Youzbashi E, Marschall M, Chaloupka I, Meier-Ewert H. 1996. Distribution of influenza C virus infection in dogs and pigs in Bavaria. Tierarztl Prax 24:337–342.
63. Horimoto T, Gen F, Murakami S, Iwatsuki-Horimoto K, Kato K, Akashi H, Hisasue M, Sakaguchi M, Kawaoka Y, Maeda K. 2014. Serological evidence of infection of dogs with human influenza viruses in Japan. Vet Rec 174:96. https://doi.org/10.1136/vr.101929.
64. Elliott RM, Yuanji G, Desselberger U. 1984. Polypeptide synthesis in MDCK cells infected with human and pig influenza C viruses. J Gen Virol 65:1873–1880. https://doi.org/10.1099/0022-1317-65-11-1873.
65. Zhang M, Hill JE, Fernando C, Alexander TW, Timsit E, Meer F, Huang Y. 2019. Respiratory viruses identified in western Canadian beef cattle by metagenomic sequencing and their association with bovine respiratory disease. Transbound Emerg Dis 66:1379–1386. https://doi.org/10.1111/tbed.13172.
66. Kimura H, Abiko C, Peng G, Muraki Y, Sugawara K, Hongo S, Kitame F, Mizuta K, Numazaki Y, Suzuki H, Nakamura K. 1997. Interspecies transmission of influenza C virus between humans and pigs. Virus Res 48:71–79. https://doi.org/10.1016/s0168-1702(96)01427-x.
67. Nissly RH, Zaman N, Ibrahim PAS, McDaniel K, Lim L, Kiser JN, Bird I, Chothe SK, Bhushan GL, Vandegrift K, Neibergs HL, Kuchipudi SV. 2020. Influenza C and D viral load in cattle correlates with bovine respiratory disease (BRD): Emerging role of orthomyxoviruses in the pathogenesis of BRD. Virology 551:10–15. https://doi.org/10.1016/j.virol.2020.08.014.
68. Yu J, Hika B, Liu R, Sheng Z, Hause BM, Li F, Wang D. 2017. The Hemagglutinin-Esterase Fusion Glycoprotein Is a Primary Determinant of the Exceptional Thermal and Acid Stability of Influenza D Virus. mSphere 2. https://doi.org/10.1128/mSphere.00254-17.
69. Song H, Qi J, Khedri Z, Diaz S, Yu H, Chen X, Varki A, Shi Y, Gao GF. 2016. An Open Receptor-Binding Cavity of Hemagglutinin-Esterase-Fusion Glycoprotein from Newly-Identified Influenza D Virus: Basis for Its Broad Cell Tropism. PLoS Pathog 12:e1005411. https://doi.org/10.1371/journal.ppat.1005411.
70. Yu J, Liu R, Zhou B, Chou T-w, Ghedin E, Sheng Z, Gao R, Zhai S-l, Wang D, Li F. 2019. Development and characterization of a reverse genetics system for influenza D virus. J Virol 93. https://doi.org/10.1128/JVI.01186-19.
71. Wan Y, Kang G, Sreenivasan C, Daharsh L, Zhang J, Fan W, Wang D, Moriyama H, Li F, Li Q. 2018. A DNA Vaccine Expressing Consensus Hemagglutinin-Esterase Fusion Protein Protected Guinea Pigs from Infection by Two Lineages of Influenza D Virus. J Virol 92. https://doi.org/10.1128/JVI.00110-18.
72. Oliva J, Mettier J, Sedano L, Delverdier M, Bourgès-Abella N, Hause B, Loupias J, Pardo I, Bleuart C, Bordignon PJ, Meunier E, Le Goffic R, Meyer G, Ducatez MF. 2020. Murine Model for the Study of Influenza D Virus. J Virol 94:e01662-19. https://doi.org/10.1128/JVI.01662-19.
73. Kaplan BS, Falkenberg S, Dassanayake R, Neill J, Velayudhan B, Li F, Vincent AL. 2021. Virus strain influenced the interspecies transmission of influenza D virus between calves and pigs. Transbound Emerg Dis 68:3396–3404. https://doi.org/10.1111/tbed.13943.
74. Sreenivasan C, Thomas M, Sheng Z, Hause BM, Collin EA, Knudsen DE, Pillatzki A, Nelson E, Wang D, Kaushik RS, Li F. 2015. Replication and Transmission of the Novel Bovine Influenza D Virus in a Guinea Pig Model. J Virol 89:11990–12001. https://doi.org/10.1128/JVI.01630-15.
75. Wang L, Chitano P, Murphy TM. 2005. Length oscillation induces force potentiation in infant guinea pig airway smooth muscle. Am J Physiol Lung Cell Mol Physiol 289:L909–15. https://doi.org/10.1152/ajplung.00128.2005.
76. Azoulay-Dupuis E, Lambre CR, Soler P, Moreau J, Thibon M. 1984. Lung alterations in guinea-pigs infected with influenza virus. J Comp Pathol 94:273–283. https://doi.org/10.1016/0021-9975(84)90046-x.
77. Reed L, Muench H. 1938. A simple method of estimating fifty percent endpoints. Am J Hyg 27:493–497. https://doi.org/10.1093/oxfordjournals.aje.a118408.
78. Herrler G, Rott R, Klenk HD, Muller HP, Shukla AK, Schauer R. 1985. The receptor-destroying enzyme of influenza C virus is neuraminate-O-acetylesterase. EMBO J 4:1503–1506. https://doi.org/10.1002/j.1460-2075.1985.tb03809.x.
79. Rogers GN, Herrler G, Paulson JC, Klenk HD. 1986. Influenza C virus uses 9-O-acetyl-N-acetylneuraminic acid as a high affinity receptor determinant for attachment to cells. J Biol Chem 261:5947–5951. https://doi.org/10.1016/S0021-9258(17)38475-2.
80. Herrler G, Reuter G, Rott R, Klenk HD, Schauer R. 1987. N-acetyl-9-O-acetylneuraminic acid, the receptor determinant for influenza C virus, is a differentiation marker on chicken erythrocytes. Biol Chem Hoppe Seyler 368:451–454. https://doi.org/10.1515/bchm3.1987.368.1.451.
81. Muchmore EA, Varki A. 1987. Selective inactivation of influenza C esterase: a probe for detecting 9-O-acetylated sialic acids. Science 236:1293–1295. https://doi.org/10.1126/science.3589663.
82. Lakdawala SS, Jayaraman A, Halpin RA, Lamirande EW, Shih AR, Stockwell TB, Lin X, Simenauer A, Hanson CT, Vogel L, Paskel M, Minai M, Moore I, Orandle M, Das SR, Wentworth DE, Sasisekharan R, Subbarao K. 2015. The soft palate is an important site of adaptation for transmissible influenza viruses. Nature 526:122–125. https://doi.org/10.1038/nature15379.
83. Mishin VP, Patel MC, Chesnokov A, De La Cruz J, Nguyen HT, Lollis L, Hodges E, Jang Y, Barnes J, Uyeki T, Davis CT, Wentworth DE, Gubareva LV. 2019. Susceptibility of Influenza A, B, C, and D Viruses to Baloxavir(1). Emerg Infect Dis 25:1969–1972. https://doi.org/10.3201/eid2510.190607.
84. Joosting AC, Head B, Bynoe ML, Tyrrell DA. 1968. Production of common colds in human volunteers by influenza C virus. Br Med J 4:153–154. https://doi.org/10.1136/bmj.4.5624.153.
85. Liener K, Durr J, Leiacker R, Rozsasi A, Keck T. 2006. Measurement of tracheal humidity and temperature. Respiration 73:324–328. https://doi.org/10.1159/000088659.
86. McFadden ER, Jr, Pichurko BM, Bowman HF, Ingenito E, Burns S, Dowling N, Solway J. 1985. Thermal mapping of the airways in humans. J Appl Physiol (1985) 58:564–570. https://doi.org/10.1152/jappl.1985.58.2.564.
87. Wang M, Veit M. 2016. Hemagglutinin-esterase-fusion (HEF) protein of influenza C virus. Protein Cell 7:28–45. https://doi.org/10.1007/s13238-015-0193-x.
88. Briscoe TA, Rehn AE, Dieni S, Duncan JR, Wlodek ME, Owens JA, Rees SM. 2004. Cardiovascular and renal disease in the adolescent guinea pig after chronic placental insufficiency. Am J Obstet Gynecol 191:847–855. https://doi.org/10.1016/j.ajog.2004.01.050.
89. Mills PG, Reed M. 1971. The onset of first oestrus in the guinea-pig and the effects of gonadotrophins and oestradiol in the immature animal. J Endocrinol 50:329–337. https://doi.org/10.1677/joe.0.0500329.
90. Ohwada K, Kitame F, Homma M. 1986. Experimental infections of dogs with type C influenza virus. Microbiol Immunol 30:451–460. https://doi.org/10.1111/j.1348-0421.1986.tb02971.x.
91. Xu H, Luo X, Qian J, Pang X, Song J, Qian G, Chen J, Chen S. 2012. FastUniq: A Fast De Novo Duplicates Removal Tool for Paired Short Reads. PLoS One 7:e52249. https://doi.org/10.1371/journal.pone.0052249.
92. Zhang Y, Aevermann BD, Anderson TK, Burke DF, Dauphin G, Gu Z, He S, Kumar S, Larsen CN, Lee AJ, Li X, Macken C, Mahaffey C, Pickett BE, Reardon B, Smith T, Stewart L, Suloway C, Sun G, Tong L, Vincent AL, Walters B, Zaremba S, Zhao H, Zhou L, Zmasek C, Klem EB, Scheuermann RH. 2017. Influenza Research Database: An integrated bioinformatics resource for influenza virus research. Nucleic Acids Res 45:D466–d474. https://doi.org/10.1093/nar/gkw857.
93. Langmead B, Salzberg SL. 2012. Fast gapped-read alignment with Bowtie 2. Nat Methods 9:357–359. https://doi.org/10.1038/nmeth.1923.
94. Anders S, Pyl PT, Huber W. 2015. HTSeq–a Python framework to work with high-throughput sequencing data. Bioinformatics 31:166–169. https://doi.org/10.1093/bioinformatics/btu638.
95. Love MI, Huber W, Anders S. 2014. Moderated estimation of fold change and dispersion for RNA-seq data with DESeq2. Genome Biol 15:550. https://doi.org/10.1186/s13059-014-0550-8.
96. Li H, Handsaker B, Wysoker A, Fennell T, Ruan J, Homer N, Marth G, Abecasis G, Durbin R, 1000 Genome Project Data Processing Subgroup. 2009. The Sequence Alignment/Map format and SAMtools. Bioinformatics 25:2078–2079. https://doi.org/10.1093/bioinformatics/btp352.
97. Organization WH. 2011. Global Influenza Surveillance Network. Manual for the laboratory diagnosis and virological surveillance of influenza. Geneva.